NTNU – Trondheim
Norwegian University of
Science and Technology

EXPERIMENTAL STUDY OF DRILLING MUD RHEOLOGY AND ITS EFFECT ON CUTTINGS TRANSPORT

Ekerette Elijah Ezekiel

Petroleum Engineering
Submission date: October 2012
Supervisor: Pål Skalle, IPT

Norwegian University of Science and Technology
Department of Petroleum Engineering and Applied Geophysics

NTNU

Norwegian University
Of Science and Technology

Faculty of Engineering
Department of Petroleum Engineering
And Applied Geophysics

EXPERIMENTAL STUDY OF DRILLING MUD RHEOLOGY AND ITS EFFECT ON CUTTINGS TRANSPORT

BY

EZEKIEL, EKERETTE ELIJAH

A Thesis submitted to the Department of Petroleum Engineering and Applied Geophysics in partial fulfillment of the requirements for the award of a degree in
Master of Science

NTNU, TRONDHEIM

NORWAY

Oct, 2012.

DEDICATION

This thesis work is dedicated to the Almighty God who gave me the wisdom, knowledge and understanding to have a successful research work.

ACKNOWLEDGEMENT

To achieve any kind of success, only personal capabilities are not sufficient. There are several factors that contribute towards achieving the end goals and objectives. Some of these factors are inspiration, guidance, moral support, motivation, initiative and encouragement. While working towards completion of this master's thesis, several individuals have made valuable and significant contributions. I would like to express my sincere gratitude to all of those individuals.

First of all, I would like to thank Associate Professor Pal Skalle, the chair of my thesis committee. Right from the beginning and throughout the entire work, his guidance, supervision, approval, untiring support and constant encouragement has been the pilot that makes this work to a success. Working with him has been a great experience. He has continuously inspired and motivated me to work toward my academic goals.

Dr. Uduak Mme, my thesis committee associate supervisor who always produced me with inspiration and built a strong desire in me to work hard to succeed. Thank you Dr. Uduak, you are a father indeed.

Dr. Francis Udoh, whose support proved to be valuable, I acknowledged you.

I am also thankful to Dr. G. T. Akpabio and Dr. E. N. Bassey for their contribution towards having a successful research work.

I would like to express my gratitude to the laboratory staff: Mr. Asangusung, Udeme and others for their support during this research work.

I am thankful to all my colleagues for their contribution. Sis Mary Isin, I acknowledge you for your contributions and prayers. Lastly, I appreciate my parents for their support towards my success in life.

ABSTRACT

Solid particles settling in drilling fluids has been one of the major problems in effective removal of drilled cuttings from the bit to the surface for a profitable drilling operation. The drag coefficient and particle Reynolds number has been reproduced experimentally and compared with theoretical work. The drag coefficient is influenced by particle size and shape, surface roughness, wall effects, turbulence intensity, fluid properties as expected.

Experiments were conducted using two types of drilling fluids, water and HEC solution of which water represented Newtonian fluid and HEC solution represented Non -Newtonian fluid. The Experiment was conducted using a cylindrical column of 1m to observe the settling rates of these particles in both fluids. Electronic stop watch was used to record the settling rates of these particles. Four cuttings sizes were used in conducting the experiment ranging from 0.055 cm to 0.692 cm with densities ranging from 2.150 g/cm^3 to 2.820 g/cm$^{3.}$ The Experiment was conducted at a room temperature of 25^o C.

The results showed lower Reynolds numbers which fall within the Laminar flow regime and could not produce higher Reynolds numbers to account for the turbulent flow regime due to experimental set up of 1m cylindrical column.

The drag coefficient decreased with increasing particle Reynolds number. Lower particles gave higher drag coefficient and lower Reynolds numbers while higher particles gave lower drag coefficient and higher Reynolds numbers in comparison for both Newtonian and Non-Newtonian fluids. The settling velocity of a given particle decreases as the fluid becomes more viscous, therefore the settling rate curve for the viscous fluid shifts downwards as the fluid viscosity increases.

Empirical correlations were developed and compared with theoretical and experimental work and it showed satisfactory agreement

TABLE OF CONTENT

LIST OF TABLES

LIST OF FIGURES

1.0 INTRODUCTION

Insufficient cleaning of the wellbore may cause several problems such as: stuck pipe, lost circulation, high torque and drag, loss of control on density and ECD's, poor cement jobs, etc. Studies on cuttings transport have been in progress since the 1940's. Initial investigation focused on terminal velocity for single phase drilling fluids, since most of the wells, terminal velocity was enough to address the problems. As interest in directional and horizontal wells increased, studies were shifted to experimental approaches and mechanistic models trying to explain transport phenomenon for all inclination angels.

One fundamental aspect in the transport of solids particles (cuttings) is the resistance force called drag force which the fluid on the particles exert, and the ability of the fluids to lift such particles which is called lift force. Both are complex functions of speed of flow, the shape of the particles, the degree of turbulence and the interaction between the particles and the pipe. Drag force is a force that acts parallel and opposite to the forward motion of the object, while the lift force exert a force normal to the motion of particles.

For the case of flow around a sphere, certain hydraulic analysis requires determining the drag coefficient as a function of particle Reynolds number. This is for example worthy to estimate the particle settling velocity, which is a parameter required for the diverse implications of cuttings particles transport and deposition in pipelines. However, most research effort report existing difficulties to model theoretically the relationship of drag coefficient.

One problem is that, the drag coefficient cannot be expressed in an analytical form in turbulent flow regime because the flow condition during the process is too complicated. This relationship can be provided experimentally in the form of charts and tables by observing the settling velocity in still fluids or by measuring the drag of spheres in the fluids. Owing to the high advances in the development of computer and software applications, the numerical data in charts and tables representing the relationship will not be practical for the fast computation of the schemes. Rather, numerical expression will be necessary. Several attempts have been made to express the relationship empirically in order to extend the range of prediction to estimate the drag coefficient versus particle Reynolds number accurately. Until now most of the empirically expressions are not satisfactory. Only few empirical attempts, although they are valid for

restricted ranges of Reynolds numbers, present accepted drag coefficient results. Most experimental work has also been directed on the determination of the drag coefficient versus particle Reynolds number. Some proved to be successful, and seemed to be accurate.

In this research work, the main focus is on Drag coefficient versus particle Reynolds number for slipping particles. The drag coefficient and Reynolds number will be reproduce experimentally. The experimental work will be compared with theoretical to understand if both of them match. Four different cuttings particles are used for the experiment. Water is used as Newtonian fluids during the experiment. Four different Power law fluids will be prepared representing the Non - Newtonian fluids. Hydroxyethyl cellulose (HEC) will be added in different proportion to change the rheology of the fluid making it a Power law fluid. The rheological parameters will be determined by a Fann Viscometer. The breakdown of the thesis in chapters is as follows:

Chapter two focused on past work done on this very topic (State of the Art).

Chapter three presents the Drag Coefficient model.

Chapter four explained all the details in the experimental investigations for this research.

Chapter five analyzed the experimental results for the Drag Coefficient versus particle Reynolds Number and Discussions.

Chapter six present quality of model, test data and future improvement.

Chapter seven presents summary and conclusion of the entire research work.

2.0 STATE OF THE ART

This chapter reviews the work done by different authors on Drag Coefficient and Particle Reynolds number for slipping particles. The views will be presented in three logical chapters for simplicity as follows:

- Particle Settling in Fluid
- Drag Coefficient versus particle Reynolds Number
- Model for predicting Drag Coefficient of a particle

2.1 PARTICLE SETTLING IN FLUID

Stoke considers the very slow flow of incompressible fluids about a solid sphere as represented by figure 2.1 below. The sphere has a radius R and diameter D. The fluid has a viscosity μ_f and the fluid density ρ_f approaches the sphere vertically upward along the negative Z- axis with uniform velocity v. Stoke gave the resultant force as:

$$F_n = \frac{4}{3}\pi R^3 \rho_f + 6\pi\mu_f R v_{sl}$$

Where:

$F_n = \text{Re}\,sul\,\text{tan}\,t\ \ force$
$R = Radius\ of\ \ the\ sphere$
$\rho_f = \ fluid\ \ density$
$g = \ \ acceleration\ due\ to\ gravity$
$\mu_f = \ fluid\ \ vis\,\text{cos}\,ity$
$v_{sl} = slip\ velocity$

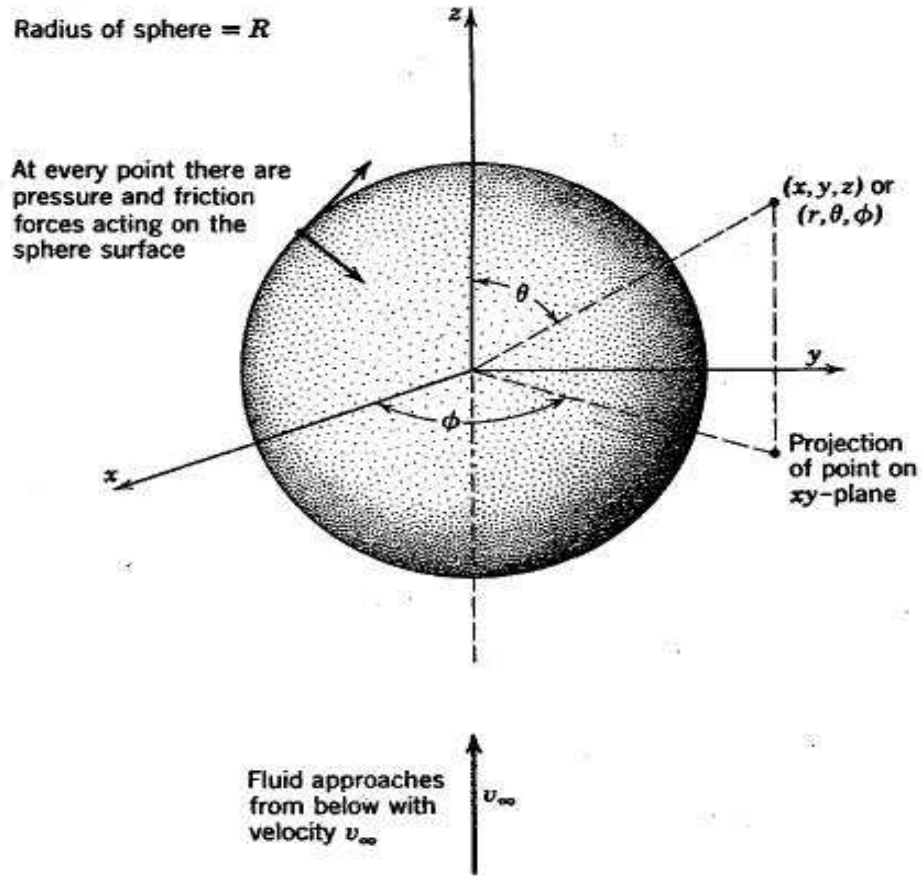

Figure 2.1: Stoke resultant force for spherical particle [Munson et al 2002].

For power-law fluids based on dimensional analysis according to Stokes, C_D is expected to be a function of the modified particle Reynolds number, N_{Rep} and the flow behaviour index n

$$C_D = f(\mathrm{Re}_p) \quad \text{.....2.2}$$

Where:

$$\mathrm{Re}_p = \frac{(10^{-3} d_s)^n v_p^{(2-n)} (10^3 \rho_f)}{k} \quad \text{.....2.3}$$

$d_s = density of\ solids$

$v_p = particle\ velocity$

$\rho_f = fluid\ density$

$\mathrm{Re}_p = Particle\ \mathrm{Re}\ ynolds\ Number$

$K = Consistency\ index$

In the laminar flow Regime where the inertia effect may be neglected, Stokes obtained the drag coefficient correlation for spherical particles within the Newtonian fluids by theoretical analysis as:

$$C_D = \frac{24}{\mathrm{Re}_p} (\mathrm{Re}_p < 0.1) \quad \text{.....2.4}$$

Pal Skalle proposed a correlation for drag coefficient and particle Reynolds number as:

$$C_D = \frac{24}{\mathrm{Re}_p} + \frac{6}{1+\mathrm{Re}_p} + 0.4 \quad \text{.....2.5}$$

Brown and Lawer correlations for drag coefficient and Reynolds number:

$$C_D = \frac{24}{\mathrm{Re}_p}(1+0.15\ \mathrm{Re}^{0.681}) + \frac{0.407}{1+8710\,\mathrm{Re}^{-1}}\ for\ \mathrm{Re} < 2x10^5 \quad \text{.....2.6}$$

Turton and Levenspiel correlations for drag coefficient and Reynolds Number:

$$C_D = \frac{24}{\mathrm{Re}_p}(1+0.173\,\mathrm{Re}^{0.657}) + \frac{0.413}{1+16300\,\mathrm{Re}^{-1.09}}\ for\ \mathrm{Re} < 2x10^5 \quad \text{.....2.7}$$

Clift et al correlations for drag coefficient and particle Reynolds number:

$$C_D = \frac{24}{R_e} + \frac{3}{16}\ for\ R_e < 0.01 \quad \text{.....2.8}$$

Pal Skalle (2005) demonstrated that when a sphere falls, it initially accelerates under the action of gravity. The resistance to motion is due to the shearing of the liquid passing around it. At some point, the resistance balances the force of gravity and the sphere falls at a constant velocity. This is the terminal velocity of the particle, defined as:

$$V_s = \frac{d^2 g(\rho_s - \rho_f)}{6\pi\mu} \qquad \text{.....2.9}$$

$V_s = slip\ velocity$
$\rho_s = density\ of\ \ spherical\ material$
$\rho_f = density\ of\ \ fluid$
$d = sphere\ diameter$
$\mu = vis\cos ity$

,

The concept of drag coefficient is normally used to define the viscous resistance as:

$$C_D = \frac{\text{Re}\, sis\tan ce\ \ force}{Dynamic\ \ pressure\ x\ \ projected\ \ Area} \qquad \text{.....2.10}$$

To calculate the Reynolds number for a particle, the settling velocity for the particle must be known and is defined as in Equation 2.9.

Particles drag coefficient and particle Reynolds number are important when we deal with the particle settling behavior. Particle Reynolds number in non-Newtonian fluid (Cho, 2001) is defined as follows:

$$\text{Re}_p = \frac{0.1617\rho v_p^{2-n} d^n}{36^{n-1} K} \qquad \text{.....2.11}$$

Where, K is consistency index of the fluid, n is fluid index behavior; Re_p is Reynolds number of the particle.

For $Re_p < 0.2$, the flow is called Stokes flow and Stokes showed that

$$C_D = \frac{24}{\mathrm{Re}_p} \qquad \text{…….....2.12}$$

For 0.2 <Re_p <500, the flow is called Allen flow and

$$C_D = 18.5\,\mathrm{Re}_p^{-0.6}$$

For 500 <Re_p<10^5, C_D = 0.44. …….....2.13

Zeidler (2002) conducted experiments with two columns: one was a clear Perspex Column (31/2 in), ID 200 cm, glass cylinder 2.36 in. To simulate the drilled cuttings and to provide the drag coefficients values over a wide range of particle Reynolds numbers, solid particles were used that varied in maximum dimensional size from 0.3 to 25 mm, with densities ranging from 2.5 to 7.8 glcm3 and in a variety of shapes e.g. spherical, disk etc.

A number of fluids were selected as the test fluids to represent three principal rheological types. The first was oil 68, which represents a Newtonian fluid; carboxyl – methyl cellulose (CMC) and Xanthan gum bio-polymer (XC) solution were used to provide power law fluids and hydroxyethyl cellulose (HEC) was used to represent a visco elastic fluid. The Rheological properties were measured with viscometer – a fann 35A to provide the data under high shear rate (170 to 1022) and low shear rate. Zeidler concluded that higher particles has lower drag with corresponding higher Reynolds number whereas lower particles has higher drag with corresponding higher drag coefficient.

Okrajni (2005) observed that when the cuttings transport phenomenon is considered, vertical slippage should be considered simultaneously. A mud in turbulent flow always induced turbulent regime of particle slippage and settling velocity decrease with increasing turbulence intensity, independent of the cuttings shape and dimensions. Therefore, in this case, the only factor that determines the particle slip velocity is the momentum forces of the mud; there is no influence of mud viscosity.

If the mud flows in the laminar regime, then depending on the cuttings shape and dimensions either turbulent or laminar regime of slippage may be expected. The laminar regime of smaller particles is mostly affected by the density and rheology of the fluid. The laminar regime of

slippage will always provide a lower value of particle slip velocity. Okrajni concluded that laminar flow usually will provide a better transport than turbulent flow.

V. C. Kelessidis and G. Mpandelis (2004) demonstrated that when a sphere is allowed to fall freely in a tube, the buoyancy and the drag forces act vertically upward where as the weight force acts downwards. At the terminal or free settling velocity in the absence of any centrifugal, electrostatic or magnetic forces

$$W = D + F_B \quad \text{.....2.14}$$

Where:

$W = weight$

$D = diameter$

$F_B = buoyancy\ \ force$

Following the work of Stokes, several models have been introduced that determines the drag coefficient as a function of Reynolds number. Heider and Levenspiel (2002) derived non linear regression from an extensive set of data points and expressions for the drag coefficient for settling in Newtonian fluids as:

$$C_D = \frac{24}{2.6}\left(1 + 0.186Re^{0.6459}\right) + \frac{0.4251}{\frac{1+6880.95}{Re}} \quad \text{.....2.15}$$

Which give a good approximation for $Re < 2.6 \times 10^5$

G. Mpandelis (2004) performed experiment using water, glycerol with a measured viscosity of 35cp and aqueous solutions of carboxyl (methyl cellulose (CMC). The solutions were prepared in batches of about 91 by adding the necessary amounts of CMC in tap water, stirring continuously for 2 hours and letting it age for 24 hours. The solution was agitated prior to each set of measurement and a small sample was taken after the experiments to determine the rheological properties using fan-viscometer.

The terminal velocity data was obtained in a cylindrical column of length of 1 m, and a diameter of 0.1 m filled with appropriate liquid. Particles were carefully dropped and readings were obtained with the use of a stop watch.

Kotthan and Tunan (2002) considered the settling of particles of different sizes with the same density. They used the Richardson Zaki correlation for the slip velocity of the particles relative to fluid and proposed that the Stokes settling velocity for a particle of different species be modified by replacing the fluid density ρ_w in buoyancy force with average density of a suspension consisting of the fluid and the particle smaller than that of species. They found very good agreement between their model and experiment.

Hannah and Harrington in (1981), conducted experimental work to determine the particle settling velocity in non-Newtonian fluids. Their experimental apparatus consisted of concentric cylinder geometry with the outer-cylinder rotating and during rotation a cutting particle was introduced and the terminal settling velocity was measured. They used hydroxyethlyl cellulose experiment. Their intent was to verify, if only knowing the shear rate, one could predict the settling velocity. They showed that by changing the viscosity term in Stokes law for a single particle settling velocity with an apparent viscosity for a given non-Newtonian fluid, the dependence on shear rate could be established. Their experimental result did not agree with the theoretical prediction using this equation and the reason for the poor fit, was poor characterization of fluid rheological properties.

Shah in (2002) presented a new approach in analyzing proppant settling data in non-Newtonian pseudoplastic fracturing fluids. He demonstrated that plotting the particle settling velocity data in a conventional manner as C_d versus N_{Rep} obscure the effect of power law flow behavior index, n. Instead he proposed plotting C_d^{2-n} versus particle Reynolds number to show the dependency of C_d on the fluid flow behavior index, n, (Figs. 2.2), significant deviation of data from the Newtonian drag curve can be seen in Fig. 2.3. The same data when plotted as $C_d^{(2-n)}$ versus N_{Rep} in Fig.2.2 show a family of curves as a function of n. Shah's work clearly reflects the dependency of the drag coefficient on both n and N_{Rep}, $C_d = f(n, N_{Rep})$.

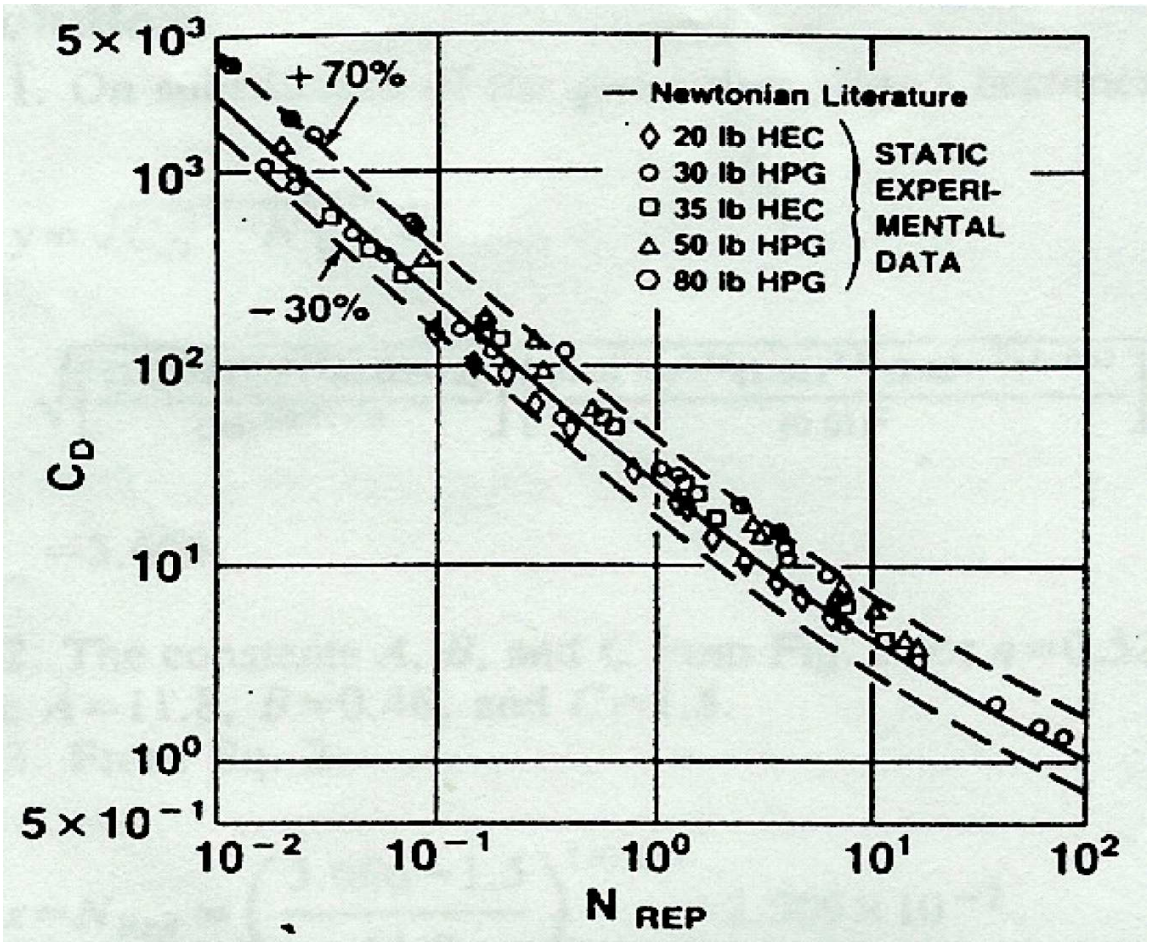

Figure 2.2: Shah's particle settling velocity data plotted as C_d versus N_{Rep} [Shah et al, 2002].

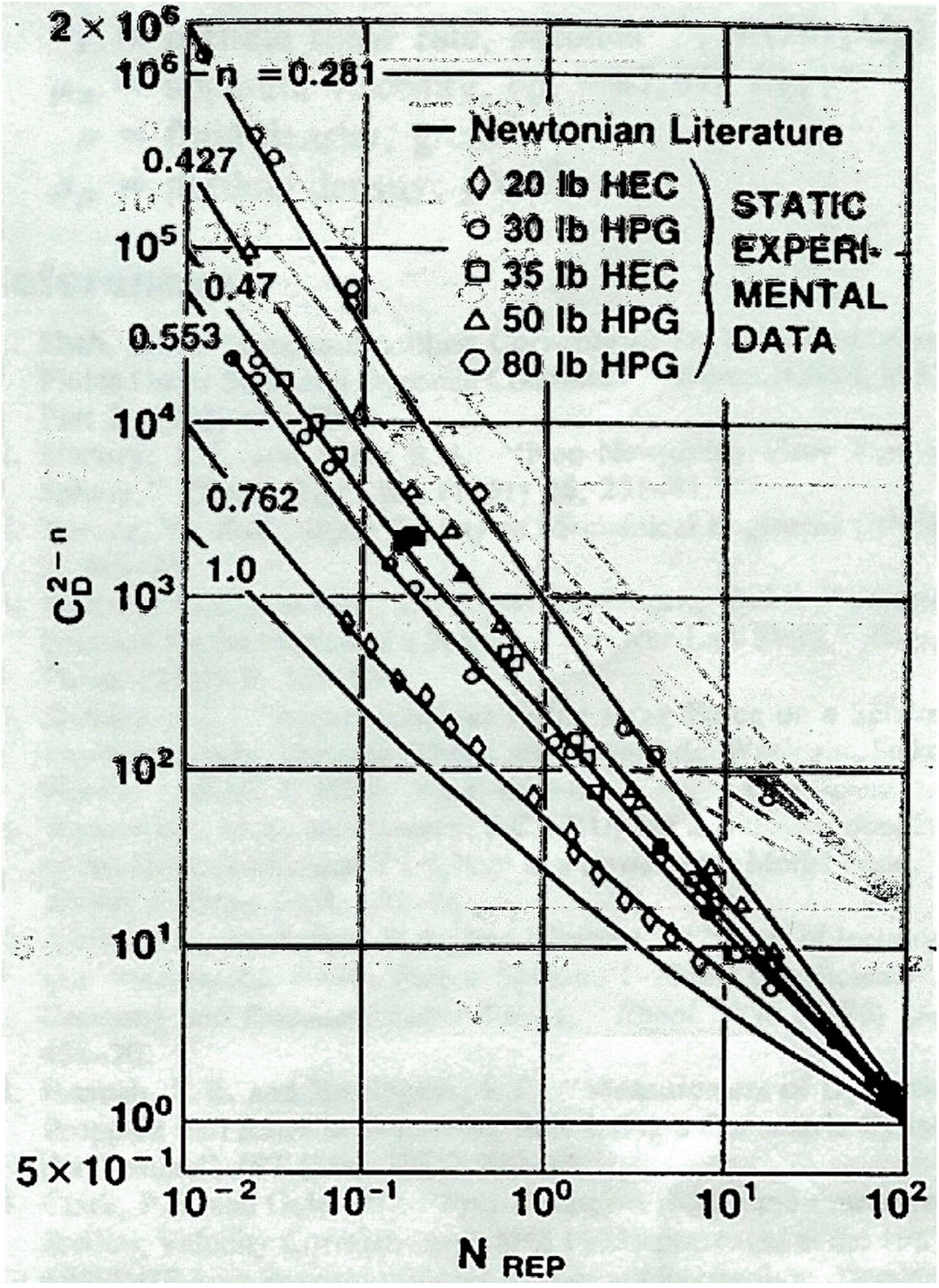

Figure 2.3 Shah's particle settling velocity data plotted as Cd^{2-n} versus N_{Rep} [Shah et al, 2002].

2.2 DRAG COEFFICIENT VERSUS PARTICLE REYNOLDS NUMBER

Richard and Walker (2001), analyzed the drag force on a particle in a flowing system generally uses a relationship between the drag coefficient C_D and particle Reynolds number N_{Rep}. The same treatment can be applied to the settling of particles in fluids. Basically, the drag coefficient represents the fraction of the kinetic energy of the settling, while the Reynolds number is a ratio between the inertia and viscous forces of a fluid. For particles with the nominal or equivalent diameter d, the drag coefficient and particle Reynolds numbers the settling is defined as:

$$C_D = \frac{1308.7d(\rho_p - \rho_f)}{V_s^{\,2}\rho_f} \qquad \text{.....2.17}$$

And

$$N_{\mathrm{Re}_p} = \frac{dv_s\rho_f}{(10.0\mu)} \qquad \text{.....2.18}$$

Where

$C_D = drag\ coefficient$
$d = particle\ diameter$
$\rho_p = density\ of\ \ particle$
$\rho_f = density\ of\ \ fluid$
$V_s = slip\ velocity$
$N_{\mathrm{Re}_p} = \mathrm{Re}\,ynold\ \ Number\ of\ \ particle$
$\mu = vis\cos ity$

The drag force consists of a viscous drag which is the result of the fluid viscosity and a profile drag which is the resistance of the fluid against the particle profile (Richard and Walker). They suggested that, A low N_{RE} (<10) implies a relatively high viscous force and a major portion of the drag force is used to overcome the viscous resistance of the fluid. At high N_{RE} (>50), the inertia force becomes dominant and the fluid density and the particle profile and surface roughness coefficient of a given particle approaches a constant value.

P. Bagchi and S. Balachandar (2003) demonstrated the case of particle settling through a turbulent flow region. They considered that the mean settling velocity of the particle provides a convenient measure of the mean drag force. In their experiment, the mean drag coefficient is computed based on the measurement of the mean settling velocity V_T and a force balance between the gravity and the drag force as:

$$C_D = \frac{4}{3} gd(\rho_f - 1)\frac{1}{V^2 t} \qquad \text{.....2.19}$$

$C_D = drag\ coefficient$
$g = acceleration\ due\ to\ gravity$
$d = sphere\ diameter$
$V_t = ter\,\min al\ velocity$
$\rho_f = density\ of\ \ fluid$

.

They demonstrated that in a turbulent flow; however there are two well understood mechanisms that influence mean settling rate. The first is due to the non linear depending of the drag on the relative velocity at finite Reynolds numbers. For the same velocity ratio and diameter d, the mean settling velocity in a turbulent flow is less than that in a stagnant flow. The settling velocity decreases with increasing turbulence intensity and the resulting mean drag as given by (2.19) is higher than that based on the terminal velocity in a stagnant flow. This effect will decrease with decreasing Reynolds number and will entirely vanish in the linear strokes limit.

Gabriel Stoke in his discovering found out that, for dilute suspensions, Stoke's law predicts the settling velocity of small spheres in fluid, either air or water. This originates due to the strength of viscous forces at the surface of the particle providing the majority of the retarded force. Stoke's law finds many applications in the natural sciences and is given by:

$$V = 2\,\frac{\left((\rho_p - \rho_f)\right)g^2}{\rho\mu} \qquad \text{.....2.20}$$

Where v is the settling velocity, ρ is density (the subscripts and f indicate particle and fluid respectively), g is the acceleration due to gravity, ρ is the radius of the particle and μ is the dynamic viscosity of the fluid.

Stoke's law applied when the Reynolds number, Re of the particle is less than 0.01. Experimentally Stoke's law is found to hold within 1% for Re $\leq$ 0.1, within 3% for Re $\leq$ 0.5 and within 9% Re $\leq$ 1.0. With increasing Reynolds numbers, Stoke Law begins to break down due to fluid inertia requiring the use of empirical solutions to calculate drag forces.

Maude and Whitmore (1999) demonstrated that, in hindered settling, the velocity gradients around each particle are affected by the presence of nearby particles. So the normal drag correlations do not apply. Also the particles in settling displace liquid which floors upward and make the particle velocity relative to the fluid greater than the absolute settling velocity. For uniform suspension, the settling velocity Vs can be estimated from the terminal velocity for an isolated particle using the empirical equation.

$$U_s - U_t\ (\varepsilon)^n \qquad \text{.....2.21}$$

Experiment 'n' changes from about 4.6 on Stokes law range to about 2.5 in the Newton; law region. For very small particles, the calculated ratio $U_s - U_t$ = 0.62 for = 0.9 and 0.095 for ε = 0.6 with large particles, the corresponding ratios are $U_s - U_t$ = 0.77 and 0.28; the hindered settling effect is not as profound because the boundary layers thickness is a smaller fraction of the particle size.

Maude and Whitmore also pointed out that if a particle of a given size are falling through a suspension of much force solids, the terminal velocity of the larger particles increased with an increased in drag coefficient.

Schiller and Naumaan (2001) conducted a research and found out that in the intermediate region between Stokes drag and Newtonian drag that, there exist a transitional regime where the analytical solution to the problem of a falling sphere becomes problematic. To solve this, empirical expressions are used to calculate drag in this region, may be valid for 0.2 $\leq$ Re $\leq$ 1000.

Stokes verified that a particle suspended in a fluid is subjected to hydrodynamic forces. For low Reynolds number, the Stokes drag force on a spherical particle is given by:

$$F_D = 3\pi\mu ud \qquad \text{.....2.22}$$

Where:

$F_D = drag\ \ force$
$\mu = vis\cos ity$
$u = velocity$
$d = particle\ diameter$

According to Stokes, equation 2.22 can be restated as:

$$C_D = \frac{F_D}{\frac{1}{2}\rho\mu^2} = \frac{24}{R_E} \qquad \text{…….. 2.23}$$

The Stokes drag is applicable to the creeping flow regime (Stokes regime) with small Reynolds number (Re < 0.5). At higher Reynolds numbers flow, the drag coefficient deviated from equation (2.22). Figure 2.4 shows the variation of the drag coefficient for sphere for a range of Reynolds numbers, See the figure below:

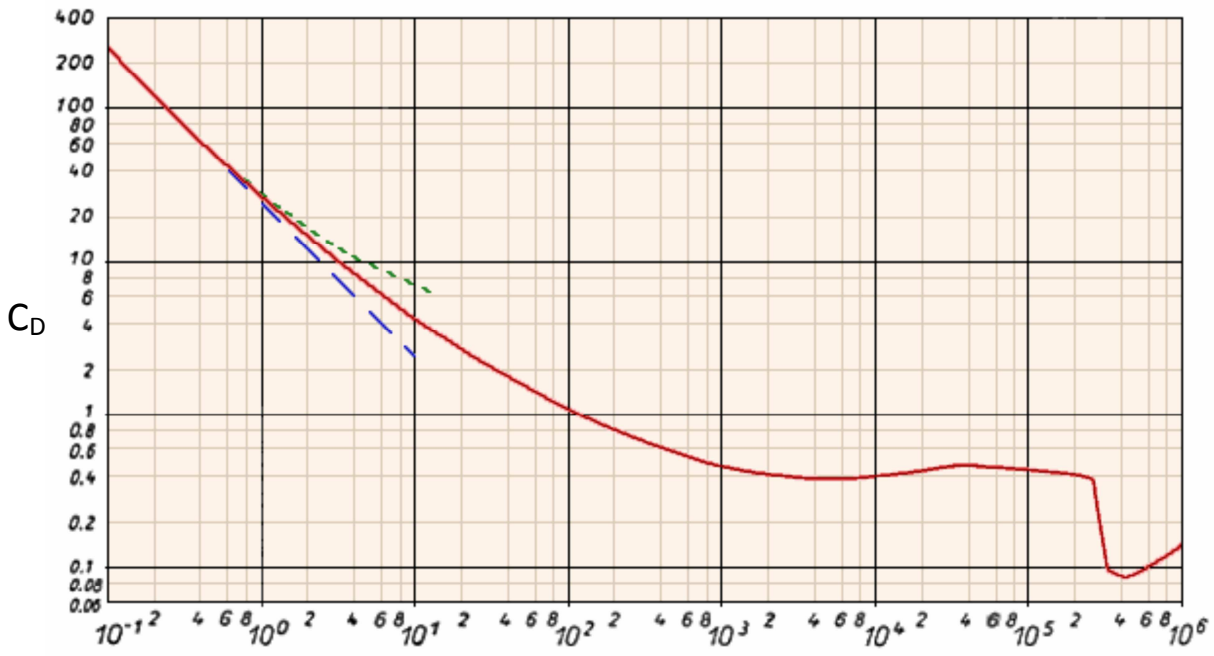

Figure 2.4: Variation of Drag Coefficient with Reynolds number for Spherical Particle [Darley et al, 1988].

Oseen (2000) included the inertia effect approximately and developed a correlation to Stokes drag given as follows:

$$C_D = \frac{24(1+\frac{3R_e}{16})}{R_e} \quad \text{.....2.26}$$

This varies for the variation of Reynolds number thus: For 1 < Re < 100, which is referred to the transitional flow region. This is shown in the figure below:

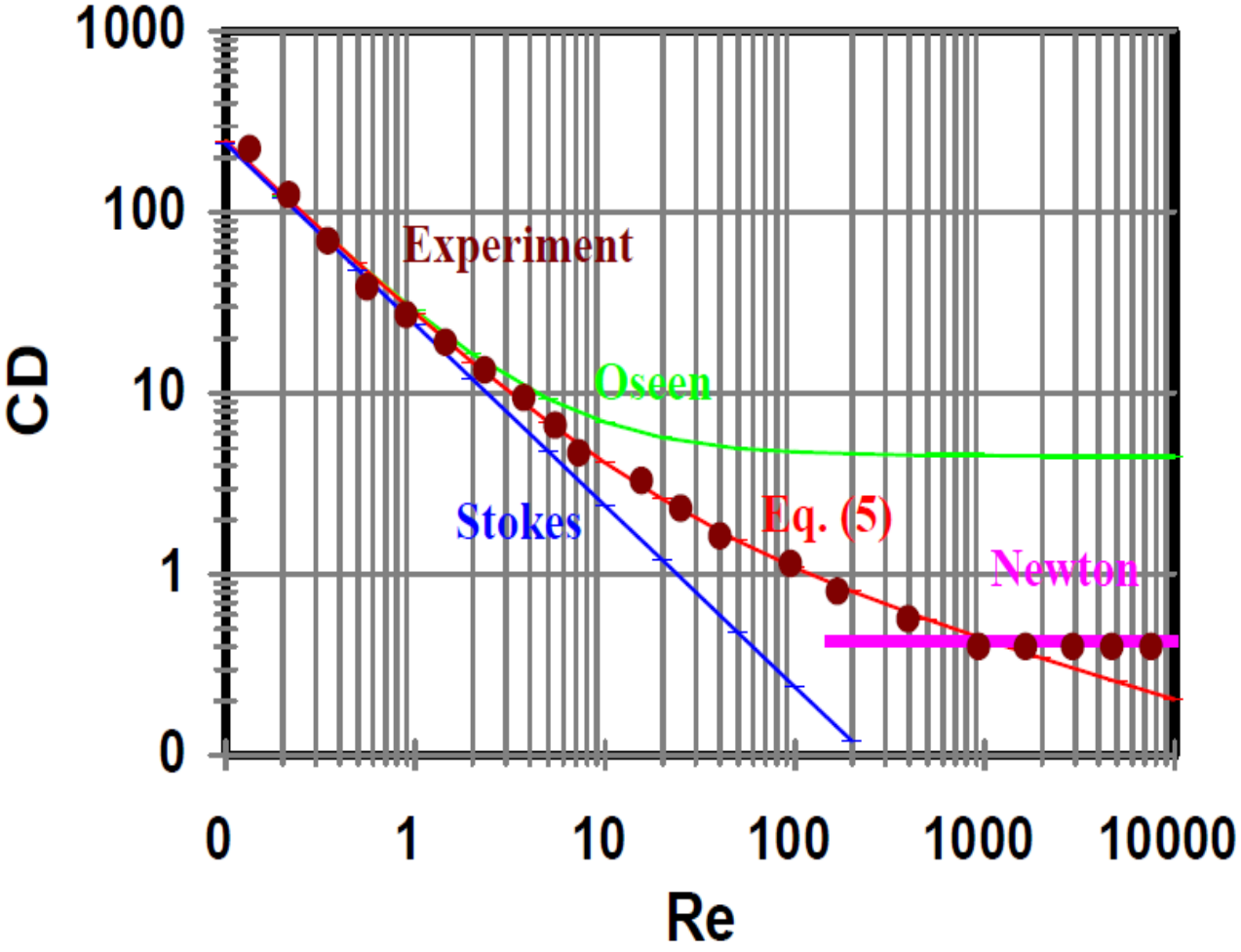

Figure 2.5: Predictions of various models for drag coefficient for spherical particle [Oseen, 2000].

For 10^3 < Re < 2.5 x 10^5, the drag coefficient is roughly constant (CD = 0.4). This regime is referred to as the Newtonian regime. At = 2.5 x 10^5 , the drag coefficient decreases sharply due to the transient from laminar to turbulent boundary layer around the sphere. That causes the separation point to shift downstream as shown in Figure 2.6

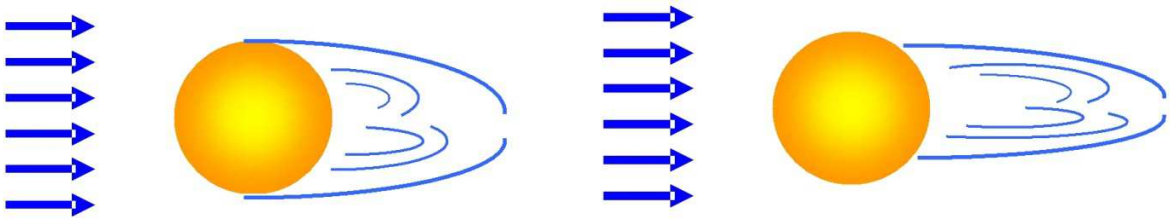

Figure 2.6: Boundary and Turbulent boundary separation [Darley et al, 1988].

For a spherical particle at very low relative velocities or very low Reynolds number (Re ≤ 1), the drag exerted on the particle is predominantly viscous drag. This region is commonly known as the creeping flow regime. The pressure distribution on an object in this region does not contribute much to the overall drag. The drag experienced by the object is due mainly to shear forces and no separation occurs around the sphere.
In the Newtonian drag regime, the drag on a sphere can be approximated by a constant, 0.44. This constant value implies that the efficiency of transfers of energy from the fluid to the particle in a Newtonian regime can again be obtained by equation the drag force to the applied force.

At moderate Reynolds numbers (1.0 < Re < 1000), both viscous and pressure drag contribute to the overall drag exerted on the sphere. Due to the presence of pressure effects, flow separation occurs in this region. The fluid stayed attached to the sphere due to increased inertia and a separation bubbles forms in the rear part of the sphere with some back flow occurring in the fluid stream.

Barnea and Migrahi (2004) performed the sedimentation of particles at higher Reynolds number in water – fluidized beds. The column used was 1 m high and 5.17 cm 1D, made of transparent plastic material. The distributor was made with a 2 cm high fixed bed of 3 mm lends shots held down by steel net and a fabric cloth. The water outlet was on one side of the column, 10 cm below the top, which was opened to allow the dropping of test particles. Glass beads of 6.35mm diameter and 2,453 kgm^{-3} density and glass beads of 800μm and 2,410 kgm^{-3} density were fluidized. Their experimental result gave n = 2.26 and μo = 0.375 ms^{-1} for the 0.635cm beads and n = 0.120 ms^{-1} for the 800 μm beads.

Evaluation of low Reynolds number of particles was effectively carried out by Rapagna (2003) by suspending glass beads in a highly-viscous liquid. The liquid (Dow corning 200 oil) has a viscosity of 12.2 Pa and a density of 975 kgm^{-13}. The diameter suspended particle was approximately 80 μm and each one weighted 2,140 kgm^{3}. These suspended particles settled only few centimeters in one hour, in sharp contrast to the settling velocity of centimeters per second achieved by the particles. The vertical sedimentation channel used in these experiments was of Plexiglas, 37 cm high and of rectangular cross-section, 8.5 cm wide and 5.5 cm deep. Each concentration of glass beads in silicon oil was thoroughly mixed in a separate container and powered into the sedimentation channel just prior to each experiment. Tests were started some minutes later after allowing entrained air to rise. The test particles were made of different materials with a high degree of spherity and a narrow diameter tolerance. Settling velocities of particles were evaluated either by measuring the time for the particle to pass by a fixed reference position with a stop watch or by filling the particle from the image taken with a high speed – video recording system.

Dallon in (2002) presented empirical correlation relating the drag coefficient of spheres falling at terminal velocity and non- Newtonian Reynolds number. He worked with hydroxyethyl cellulose (HEC), carboxymethyl cellulose (CMC), and polyethylene oxide (PEO), covering the power law behaviour index, n, ranging from 0.63 to 0.94 and particle Reynolds number between 0.016 and 500, and drag coefficient between 0.46 - 1400. Larger particles diameter are seen to have higher settling velocities than smallers. The equation uses two empirical coefficients and the procedure for their determination is provided. One of the draw backs of this equation is the use of trial and error solution for terminal velocity determination. Poor results are found between the experimental data and theoretical predications.

2.3 MODEL FOR PREDICTING DRAG COEFFICIENT OF A PARTICLE

Chabra in (1990) attempted to obtain a unified model to predict the drag coefficient of a falling sphere in a power law fluid. Thus, he used his data along with all of Dallon, Prakash, and Lali et al for analysis. The common ground between all these authors was that they plotted their experimental data on a logarithmic paper as the drag coefficient versus particle Reynolds number, Figs 2.7 through 2.8 show these plots. Most of the data points fell along the Newtonian drag curve and the others were considered as scatter with 18% deviation from the Newtonian drag curve. These results have led Chabra to conclude that

the standard curve available for Newtonian fluids provides an “adequate” representation for power law fluids without any dependence on power law flow behavior index, n, within the following ranges:

$1 < N_{Rep} < 1000$ and $0.535 < n < 1$.

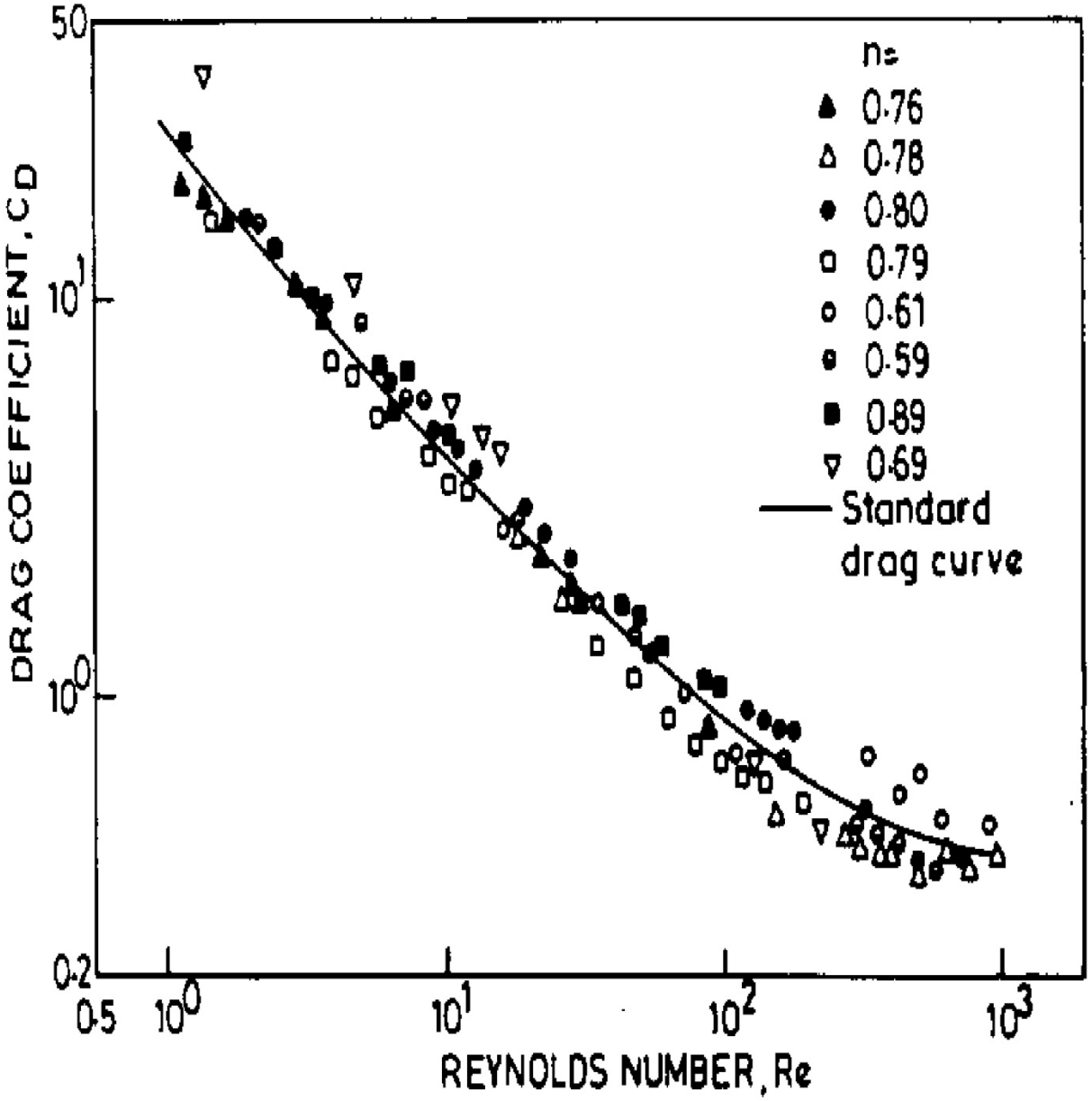

Figure 2.7: Chhabra's data compared with the Newtonian drag curve [Chhabra, 1990].

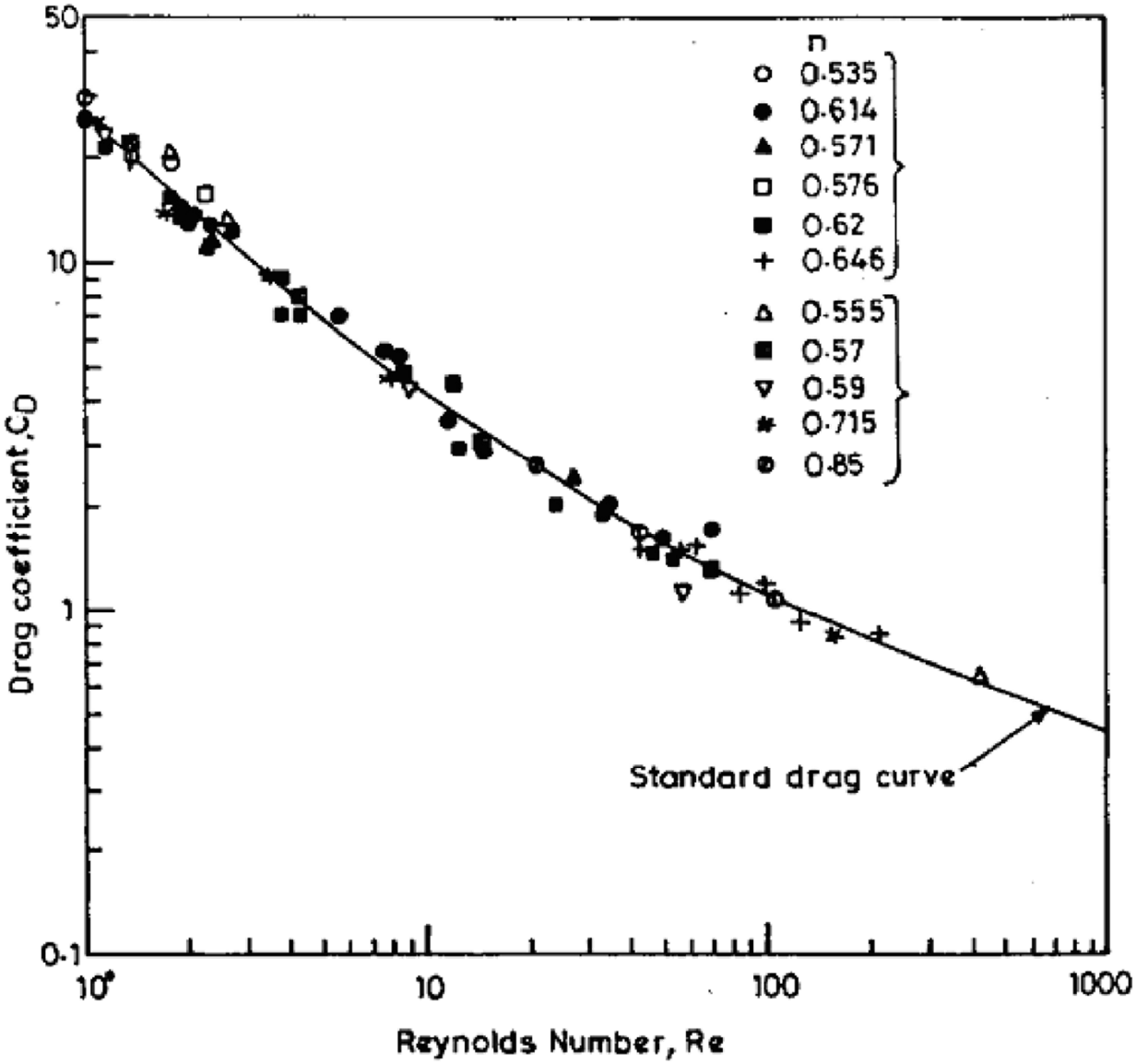

Figure 2.8: Prakash and Lali et al.'s data compared with the Newtonian drag curve [Chhabra, 1990]

3.0 MODEL OF THE PROBLEM

This present study covers basic principles for spherical particles settling in a stagnant fluid. The method involves careful dropping the cuttings particles in the fluid and simultaneously noting the actual time it take the particles to settle down in the fluid.

This model is a physical model. It is formulated based on the Archimedes principles of motion which states that, when a body is wholly or partially immersed in a fluid, it experiences an upthrust equal to the weight of the fluid downward. The model is formulated from a detailed investigation on the physics behind the cuttings particles settling in fluid as observed from the experiment. This is done by taking a critical look of the forces acting on a particle when emerged in the fluid. The forces acting on the falling cutting particle could be analyzed as follows:

When an object is dropped inside a viscous fluid, it is influence of three forces.

- Its weight acting downward
- The viscous force of the fluid acting upward
- the upthrust of the fluid on the object acting upwards

At first, the weight of the body (the downward force) is greater than the sum force thus upward. The resultant downward force thus causing the object to accelerate (increase its velocity with time). After sometimes, the two forces acting upwards become equal to the weight of the object acting downwards. At this point, the resultant force on the body becomes zero and the body ceases to accelerate. This velocity of the body attained when acceleration is zero is called terminal velocity (v_t).

In the discussion above, we analysed the physics behind cuttings particles when emerged in a particular fluid. In this section, we will look at the mathematical development of this model from a force balance of all the forces acting on the particle settling. Also, we will develop model for the settling velocity and empirical corrections for laminar, Transitional, turbulent settling velocity and empirical correlations. The following assumptions are considered in the development of the model.

- The particle is a solid sphere.
- The particle is far from the vessel wall so that flow pattern around the particle is not distorted.
- The fluid is stationary
- The particle is moving at its terminal velocity with respect to the fluid.

3.1 MODEL DEVELOPMENT

Taking a look at simple force balance of cutting particle emerged in stationary fluids.

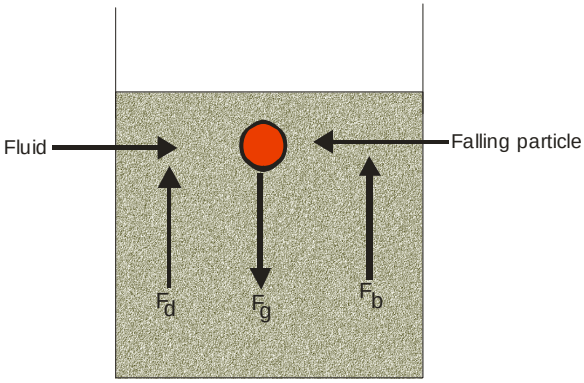

Figure 3.3.2 Particle settling in fluid

When these particles settled at terminal velocity (v_p), a force is established between drag force, gravity, and buoyancy force.

$$F_{drag} + F_{gravity} + F_{buoyancy} = 0$$

$$F_{drag} = -(F_{gravity} + F_{buoyancy),} =$$

Net weight of the particle.

Now: $F_D = -(\rho_p v_p - (g) + \rho_f v_p g) = \Delta\rho v g$ …….3.1

In equation (3.1), $\Delta\rho = \rho_s - \rho_f$ is the solid fluid density difference.

The equation shows that the drag force for a particle settling is known before hand, once its volume and the density difference of the fluid are known, for a spherical particle.

$V_P = \frac{4}{3}\pi R^3$,so that …… 3.2

$F_D = \frac{4}{3}\pi R^3 \Delta\rho g$ ……3.3

The drag coefficient therefore is equals to:

$$C_D = \frac{F_D}{\frac{1}{2}\rho_f v_s^{\,2}\pi R^2} = \frac{4}{3}\frac{\Delta dg}{\rho_f v^2} \text{ ……..3.4}$$

$$C_D = \frac{4}{3}\frac{\Delta dg}{\rho_f v^2} \text{ ……..3.5}$$

Where the sphere diameter is d = 2R

$$\Delta = \frac{\rho_s}{\rho_f} - 1$$

$v_s = ter\,\min al\ velocity$

$\rho_f = density\ of\ \ fluid$

$C_D = drag\ coefficient$

$g = acceleration\ due\ to\ gravity$

3.2 LAMINAR AND TURBULENT FLOW SETTLING VELOCITY

Assuming there are two major equations of the settling velocity depending on the particle Reynolds number as follows:

C_D = $\frac{A}{Re}$ when R <1 (Laminar flow) …….. 3.6

C_D = B when 10^5 < Re < 2 x 10^5 (turbulent flow) ……...3.7

Where:

C_D: drag coefficient

A and B are constants

Then, from an extension of equation (3.1),

If we write equation (3.1) as:

$$C_D = \frac{4}{3}\frac{gd}{v_{s^2}} \qquad \text{……3.8}$$

We can form the following relationship for the Laminar Flow region:

$$V_S = \frac{4}{3A}\frac{gd}{v} \qquad \text{…… …….. …… ……3.9}$$

Likewise, the turbulent flow setting velocity can be expressed as:

$$V_S = \sqrt{\frac{4}{3B}\Delta gd} \qquad \text{……3.10}$$

Where:

V_S = settling velocity

g = acceleration due to gravity

d = Particle diameter

A = 24

B = 0.4

If C_D and R_E are related such that:

$C_D = \left[\left(\frac{A}{R_e}\right)^{1/n} + B\frac{1}{n}\right]^n$ ……3.11

Where n is an exponent.

Assuming, there exist a dimensionless particle diameter, and then we can obtain a relationship defined as:

$D^* = \left(\frac{\Delta g}{v^2}\right)^{1/3} d$ ……3.12

Where d* = dimensionless particle diameter. This definition is in cooperated with equation (3.1) , the relationship between drag resistance and dimensionless particle diameter can be expressed as:

$C_D = \frac{4}{3}\frac{d^{*3}}{Re^2}$ ……3.13

Finally, the settling velocity can be calculated when equation (4) and (6) are combined as:

$V_s = \frac{V}{d}\left[\sqrt{\frac{1}{4}\left(\frac{A}{B}\right)^{2/n} + \left(\frac{4}{3}\frac{d^{*3}}{B}\right)^{1/n}} - \frac{1}{2}\left(\frac{A}{B}\right)^{1/n}\right]^n$ ……..3.14

Where Vs = Settling velocity

D= Particle diameter

d*= dimensionless particle diameter

A= Constant = 24

n = 2

3.2.1 THEORETICAL EMPIRICAL CORRELATION FOR LAMINAR FLOW REGIME:

In the laminar flow regions, where the inertia effect may be neglected, Stokes obtained the drag coefficient correlations for spherical particle in Newtonian fluids as:

$C_D = \frac{24}{Re}\ for\ R_e < 1$

Clift *et. al.* empirical correlations for the laminar flow region is:

$\frac{24}{R_e} + \frac{3}{16}$ For $R_e < 0.01$ ……..3.15

And:

$\frac{24}{R_e} + 1 + 0.1935\ R_e^{0.6305}$ For $20 < R_e \leq 260$……..3.16

3.2.2 THEORETICAL CORRELATION FOR TRANSITIONAL FLOW REGIME:

For the Transitional flow Region, Stoke obtained an empirical correlation as:

$C_D = \frac{18.5}{Re^{0.6}}$ for $1 < R_e < 500$…… 3.17

Clift *et al.* obtained an empirical correlation for the transitional flow region as:

$C_D = 10^{1.6435-1-.122 \log R_e + 0.1558\, log^2 R_e}$……3.18

Allen obtained on empirical correlation for the transitional flow as:

$C_D = \frac{30.5}{Rep^{0.6}}$ for $1 < Re < 1000$……...3.19

3.2.3 THEORETICAL CORRELATION FOR TURBULENT FLOW REGIME:

For the turbulent flow region, Stoke obtained empirical correlation based on the application of Newton's Law as:

$C_D = 0.44$ for $1000 < R_e < 2 \times 10^5$……3.20

Turton and Levenspiel obtained an empirical correlation as:

$C_D = \frac{24}{R_e}(1 + 0.173R_e^{0.657}) + \frac{0.413}{1+16300\, R_e^{-1.09}}$ for $R_e < 2 \times 10^5$……3.21

Brown and Lawler obtained an empirical correction for the turbulent region as:

$C_D = \frac{24}{R_e}\left(1 + 0.15{R_e}^{0.681}\right) + \frac{0.407}{1+8710R_e^{-1}}\ for\ R_e < 2\ x\ 10^5$……3.22

Pal Skalle obtained a general correlation for drag coefficient and particle Reynolds number in Newtonian fluids as:

$C_D = \frac{24}{R_e} + \frac{0.6}{1+Rep} + 0.4$……3.23

3.3 PRESENT PREDICTION OF EMPIRICAL CORRELATION FOR DRAG COEFFICIENT AND PARTICLE REYNOLDS NUMBER

These present predictions are based on an extension of the work done by some researchers from the existed model as highlighted in section 3.1 to section 3.2.

3.3.1 LAMINAR FLOW REGIME

Stoke's correction for the laminar flow region did not take into account the wall effect on particle setting.

If we now take into account, the effect of the wall, one can analyzed the drag acting on a particle moving towards a wall developing a new empirical correlation under laminar flow condition as:

$C_D = \frac{24}{R_e}\left(1 + \frac{d}{2h}\right)$ for $R_e < 1$ ……3.24

Where

C_D = Drag coefficient

R_e = Reynolds number

d = Particle diameter

h = Distance from the wall.

3.3.2 TRANSITIONAL FLOW REGIME:

For the transitional flow region, if one takes into account a higher Reynolds number, a new correlation can be developed as:

$$C_D = \frac{23.8}{Rep^{0.7}} \; for \; 1 < R_e < 1000 \quad \text{.....3.25}$$

3.3.3 TURBULENT FLOW REGIME

At a very high Reynolds number, example $2x10^5$, the drag coefficient will fall dramatically giving rise to 0.10 instead of 0.44.

A general correlation for the drag coefficient and particle Reynolds number can be formulated as an extension of done by Pal Skalle in the theory as:

$$C_D = \frac{24}{R_e} + \frac{0.8}{1+Rep} + 0.6$$

4.0 EXPERIMENTAL WORK

This Chapter explains all the experimental investigations carried out in the course of this research work.

4.1 CLASSIFICATION OF CUTTINGS SIZES

The parameter involved in the study of the settling velocity, drag coefficient and particle Reynolds numbers pertaining to solid particles is the particle diameter. The cuttings sizes used in this research work were gotten from Norway.

Table 4.1: Classification of cuttings sizes

Source	Particle size	Particle diameter, cm
Norway	Very small	0.055
Norway	Small	0.224
Norway	Large	0.465
Norway	Very large	0.692

The particle diameters were measured using venire caliper.

4.2 EXPERIMENTAL APPARATUS

Certain laboratory apparatus were used to perform this very experiment and there are as follows:

Glass cylinder (1m), Mud balance, Mixer, Stirring rod, measuring cup, Sieve, Fann Viscometer, Venire Caliper and stop watch.

4.3 TEST MATRIX FOR THE CUTTINGS PARTICLES

Table 4.3: Test matrix for cutting sizes

Particle Sizes (cm)	Shape	Density ρ (g/cm^3)
0.055	Spherical	2.150
0.224	Spherical	2.232
0.465	Spherical	2.449
0.692	Spherical	2.820

The particle densities were determined by first measuring the mass of each cutting particle on an electronic scale . It was then divided by the volume of each sphere.

4.3.1 TEST MATRIX FOR THE THEORETICAL

Table 4.3.1: Test matrix for the theoretical [Munson, et al 2002].

Particle sizes (cm)	Shape	Densities (g/cm^3)
0.122	Sperical	2.314
0.316	Spherical	2.328
0.345	Spherical	2.541
0.575	Spherical	2.670

4.4 FLUID RHEOLOGICAL PROPERTIES

4.4.1 NEWTONIAN FLUIDS:

Water was used as Newtonian fluid

Table 4.4.1 Rheological properties for Newtonian Fluid

Fluid	Viscosity	Fluid density
Water	1 cp	1 g/cm^3

4.4.2 NON NEWTONIAN FLUID PREPARATION:

Four HEC solutions were prepared to create power law fluids by weighing the correct amount of HEC and adding it to the vessel already filled with the proper amount of water and allowed to agitate. Agitations continued for about one hour after addition and the mixture was left for 24 hours for complete hydration. Before testing, the mixture was agitated for 10 minutes, a sample was taken for rheological measurement and the test started.

The density of each fluid model was measured by using Faan scale mud balanced equipment which is known to be accurate and self contained measuring device.

All the fann measurements as used in this experiment are presented below:

Table 4.4.2 Viscometer readings for 0.5wt% liquid HEC Polymer fluids

RPM	SHEAR STRESS (S^{-1})	DIAL READING (θ)	SHEAR RATE (τ) Ib/100ft^2	SHEAR RATE(τ) Pa
600	1022	35	37.1	17.76
300	511	26	27.56	13.20
200	341	24	25.44	12.18
100	170	15	15.9	7.61
6	10	9	9.54	4.57
3	5	7	7.42	3.55

Table 4.4.3 Viscometer readings for 1.5wt% liquid HEC Polymer fluids

RPM	SHEAR STRESS (S^{-1})	DIAL READING (θ)	SHEAR RATE (τ) Ib/100ft^2	SHEAR RATE(τ) Pa
600	1022	38	40.28	19.28
300	511	28	29.68	14.20
200	341	25	26.50	12.68
100	170	17	18.02	8.62
6	10	11	11.66	5.58
3	5	11	11.66	5.58

Table 4.4.4 Viscometer readings for 2.5wt% liquid HEC Polymer fluids

RPM	SHEAR STRESS (S^{-1})	DIAL READING (θ)	SHEAR RATE (τ) Ib/100ft^2	SHEAR RATE(τ) Pa
600	1022	44.2	46.85	22.43
300	511	30.5	32.33	15.47
200	341	26.2	27.77	13.30
100	170	18.50	19.61	9.39
6	10	12.12	12.84	6.15
3	5	11.58	12.27	5.87

Table 4.4.5 Viscometer readings for 5.0wt% liquid HEC Polymer fluids

RPM	SHEAR STRESS (S^{-1})	DIAL READING (θ)	SHEAR RATE (τ) Ib/100ft^2	SHEAR RATE(τ) Pa
600	1022	56.5	59.89	28.68
300	511	38.1	40.39	19.34
200	341	33.3	35.30	16.90
100	170	24.6	26.07	12.49
6	10	15.2	16.11	7.71
3	5	9.8	10.39	4.97

All measurements were done at a room temperature of 25^0C

Table 4.4.6 Calculated values for rheological model for the four power law fluids

Fluid	Rheology Model	Fluid Behavior Index, n	Consistency Index, K
Fluid 1: HEC, 5g/liter	Power Law	0.568	0.547
Fluid 2:HEC, 2,5g/liter	Power Law	0.536	0.560
Fluid 3:HEC,1,5g/liter	Power Law	0.441	0.907
Fluid 4:HEC,0.5g/liter	Power Law	0.428	0.910

4.5 TEST PROCEDURES

The following test procedures were applied when running the experiments:

- Mesh sieve of various sizes along with Venire Caliper was used in order to know the cutting sizes.
- The glass tube was properly calibrated from 0 to 1m (100cm)
- The glass tube was then filled with fluid to a 100cm mark
- After filling the glass tube with fluid, it was mounted on a table
- Cutting particles were then dropped into the glass tube carefully and gently
- The Stop watch was simultaneously started to record the actual time the particles take to settle down.
- Particles were allowed to settled at the 100 cm mark in order to reach its terminal velocity
- For each particle size, the experiment was repeated for five times in order to avoid error
- The terminal velocity was then calculated
- This same procedure was carried out for all the particles settling both in Newtonian and non Newtonian fluids.

Figure 4.5.1: Pictures of Experimental Set up

5.0 RESULTING DRAG COEFFICIENT VERSUS REYNOLDS NUMBER CHARTS:

This chapter shows all the results obtained as a result of the experiment run. The results are Presented in tables located in Appendix A. The graphical representations of the results are Shown below logically according to each particle size in a particular fluid.

(a) 0.692 cm Particle in Newtonian Fluids

The result obtained from the experimental for this particle is presentable in table 5.1 located in the appendix A. The table is used to plot figure 5.1 as shown below:

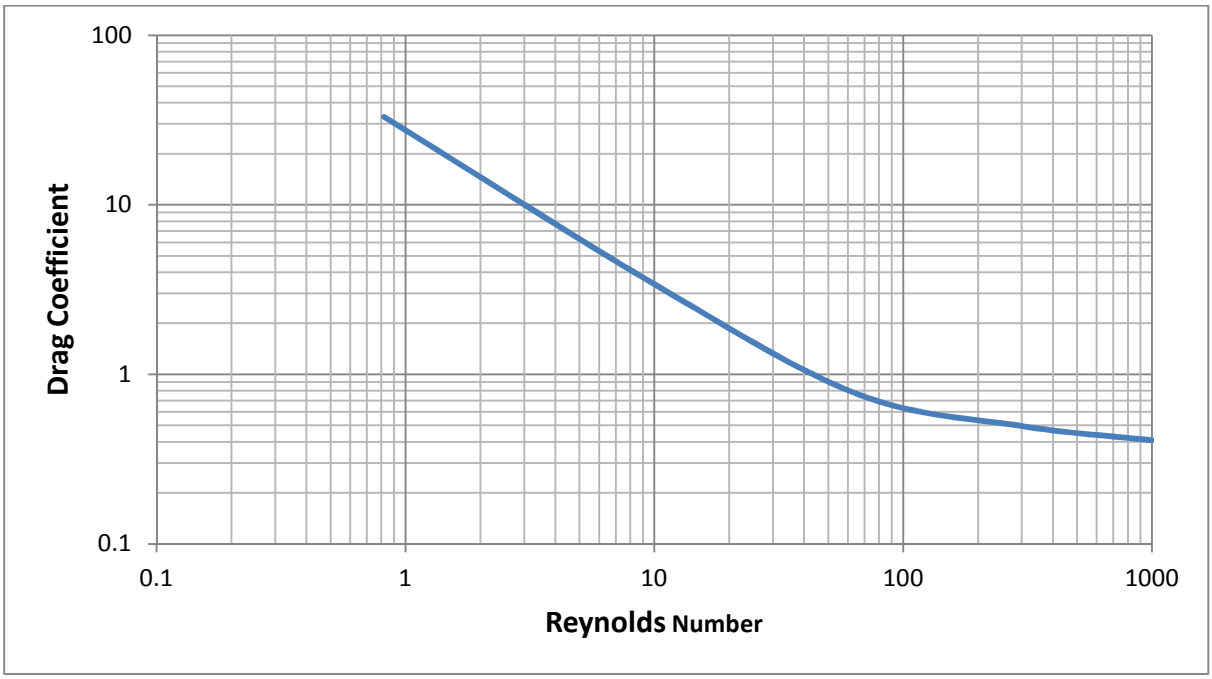

Figure 5.1: Drag Coefficient versus Particle Reynolds Number for 0.692cm particle in Newtonian fluids

(b) 0.692 cm particle in Non Newtonian fluids

The result obtained from the experimental for this particle is presented in table 5.2 located in the appendix A. The table is used to plot figure 5.2 as shown below:

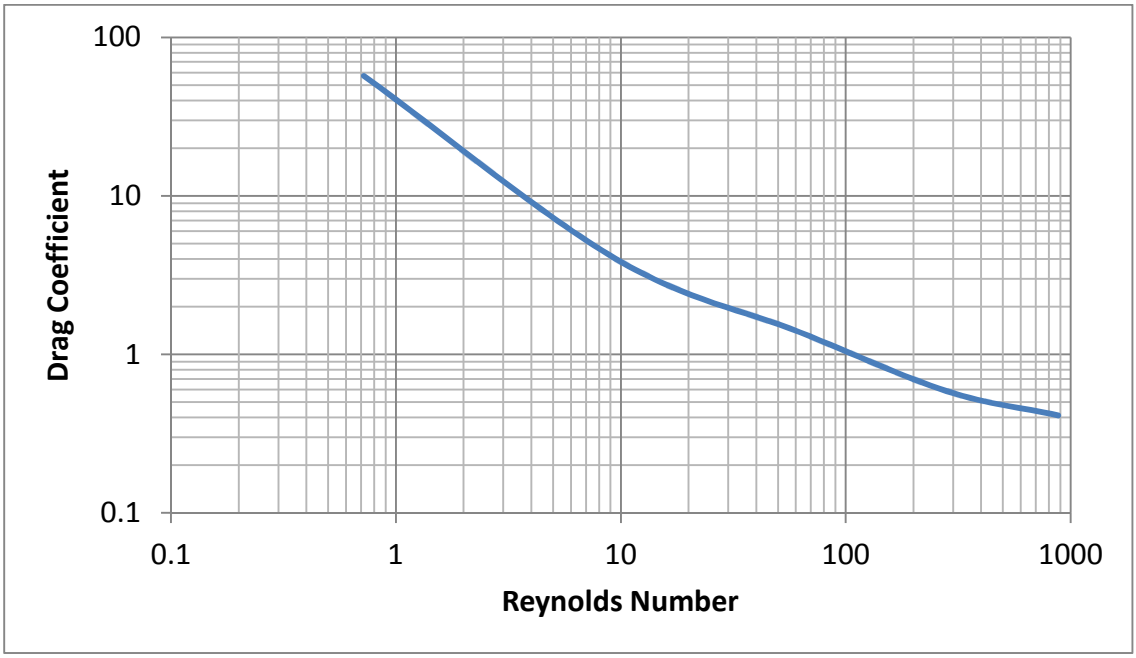

Figure 5.2: drag Coefficient versus Reynolds number for 0.692 cm in Non-Newtonian

(C) 0.465 cm particle in Newtonian fluids

The results obtained from the experiment for this particular particle is shown in table 5.3 as located in Appendix A. The graph below represents the results presented in the same table

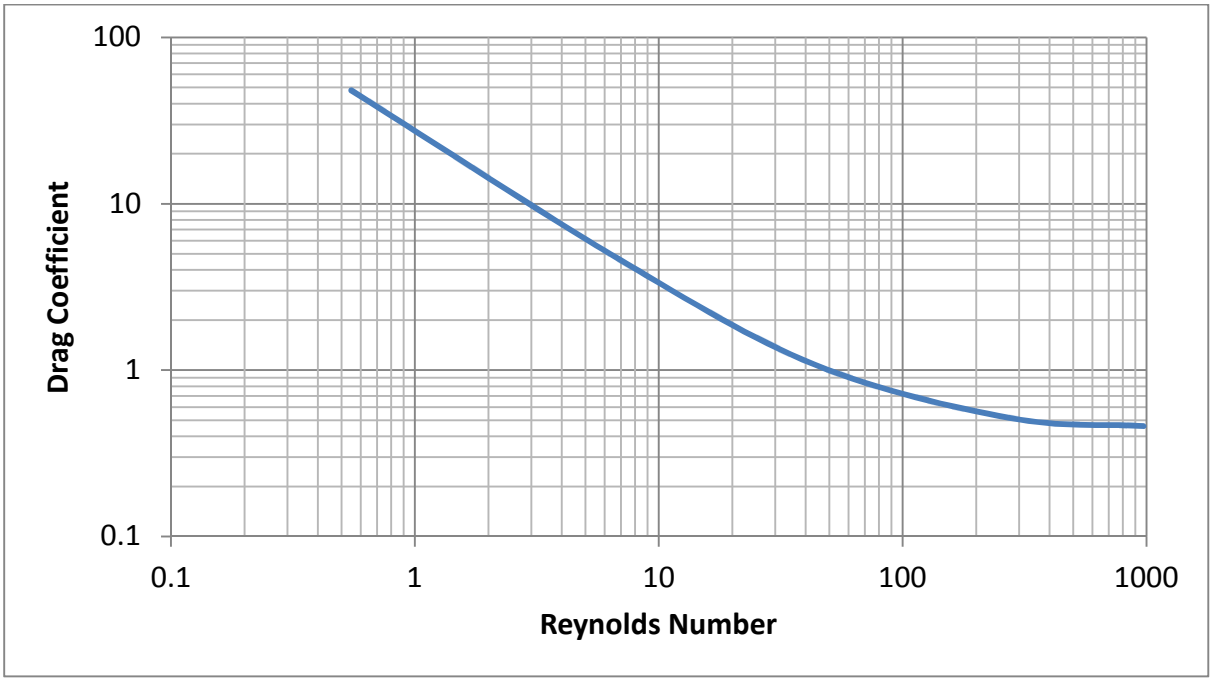

Figure 5.3: Drag Coefficient versus Particle Reynolds Number for 0.465cm particle in Newtonian fluids

(d) 0.465cm particle in Non Newtonian fluids

The experimental result of this particle is presented on table 5.4 which is viable at Appendix.

The figure showing the plot from this table is shown below:

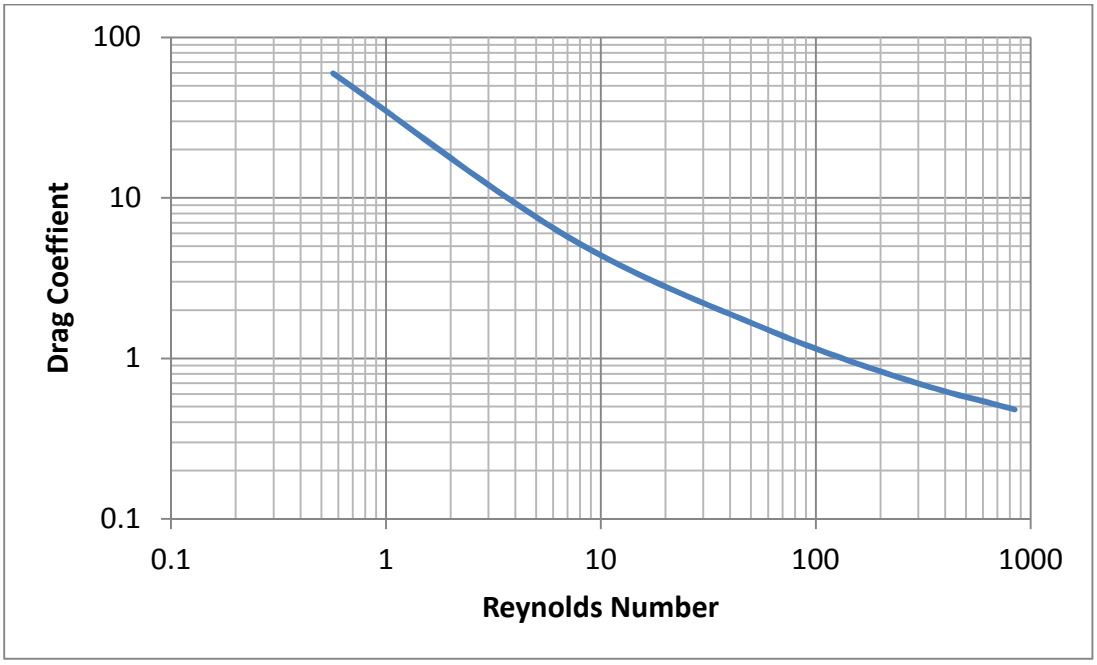

Figure 5.4: Drag Coefficient versus Particle Reynolds Number for 0.465cm particle in Non -Newtonian fluids

(e) 0.224 cm particle in Newtonian fluids

The presentation of this result is seen in table 5.5 located on Appendix A. The plots made out of this table is seen below:

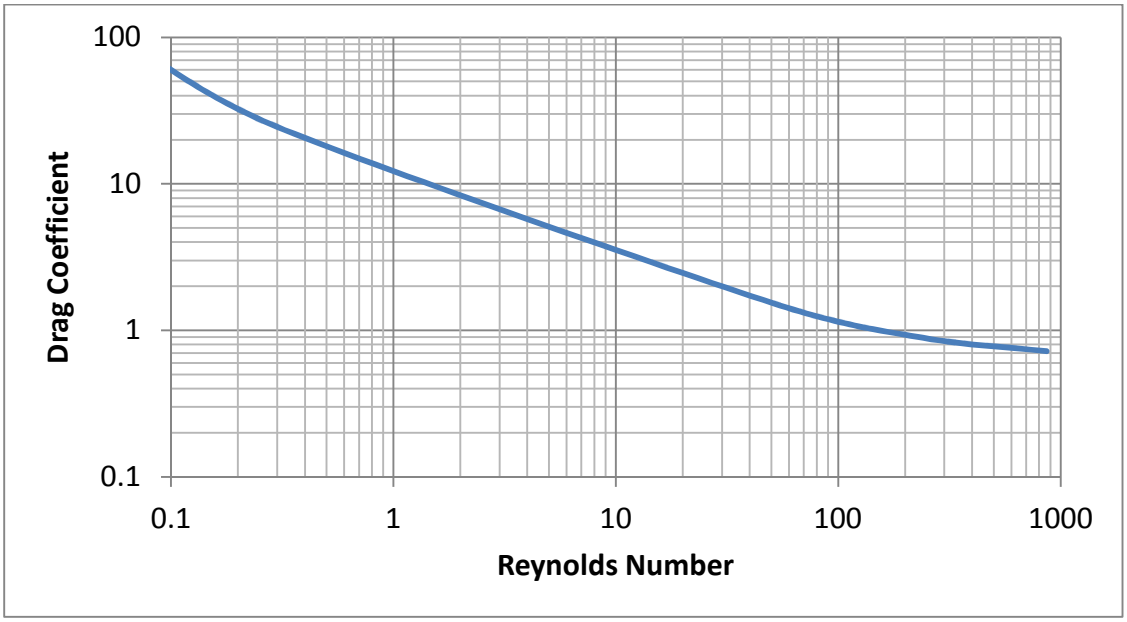

Figure 5.5: Drag Coefficient versus Reynolds number for 0.224cm particle in Newtonian

(f) 0.224 cm Particle in Non Newtonian fluids

The experimental values obtained from this particle is visible on table 5.6 which is found in Appendix A. Below is the figure plotted from this particular table

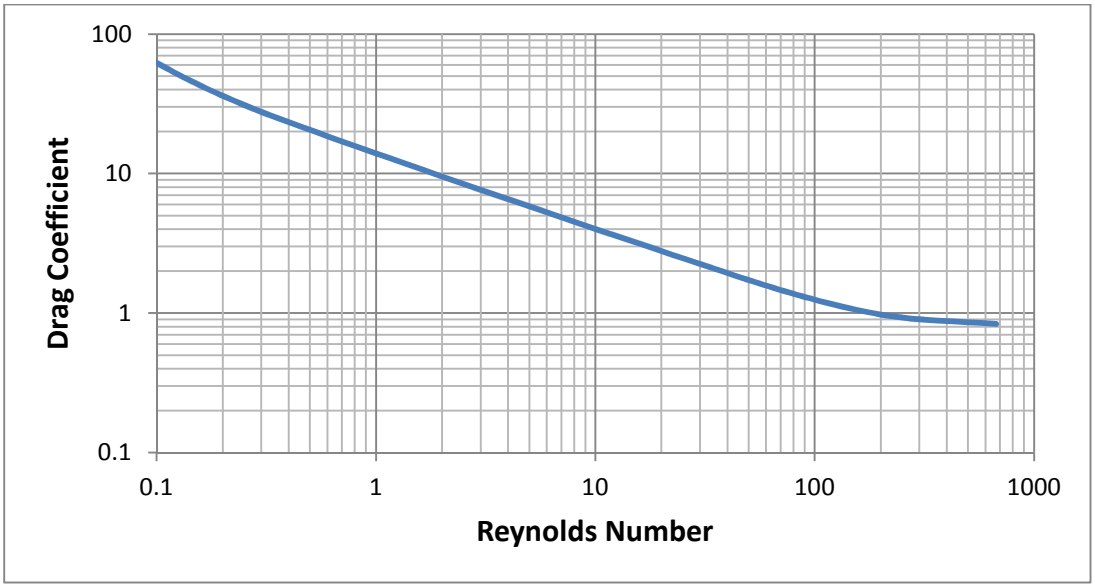

Figure 5.6: Drag Coefficient versus Particle Reynolds Number for 0.224 cm particle in Non-Newtonian fluids

(g) 0.055 cm particle in Newtonian Fluids

The results obtained from 0.055 cm particle in Newtonian fluids is located on table 5.7 as it is found in Appendix A. The graphical presentation of this result plotted from this table is shown below:

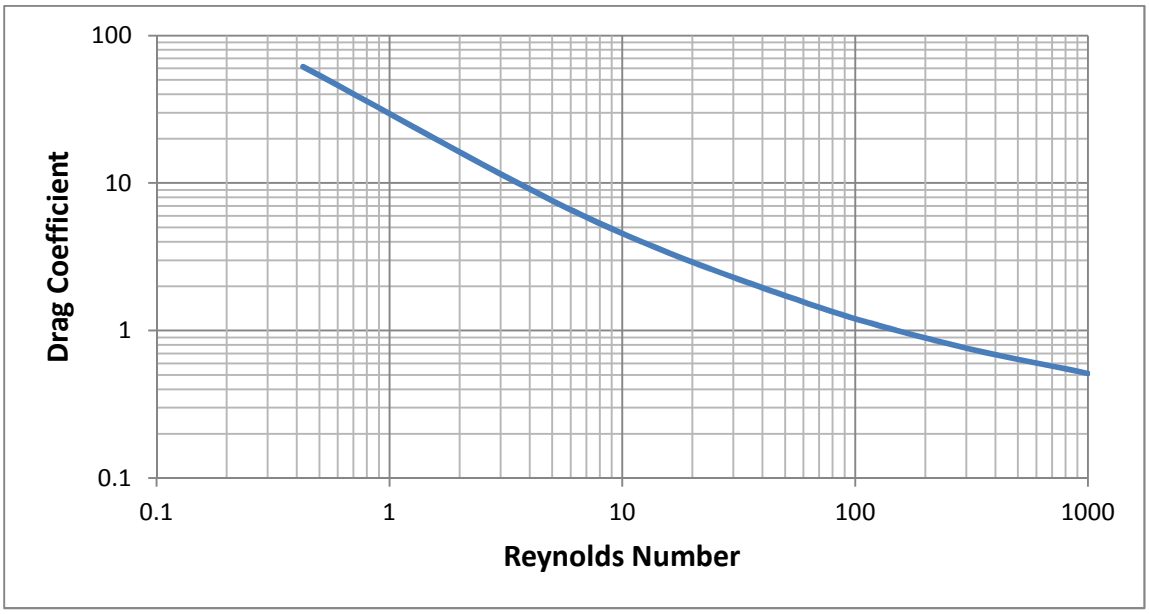

Figure 5.7: Drag Coefficient versus Particle Reynolds Number for 0.055 cm particle in Newtonian fluids

(h) 0.055 cm particle in non Newtonian fluids

This result is shown on table 5.8 which is located at Appendix A. The figure shown below is is plotted from this table:

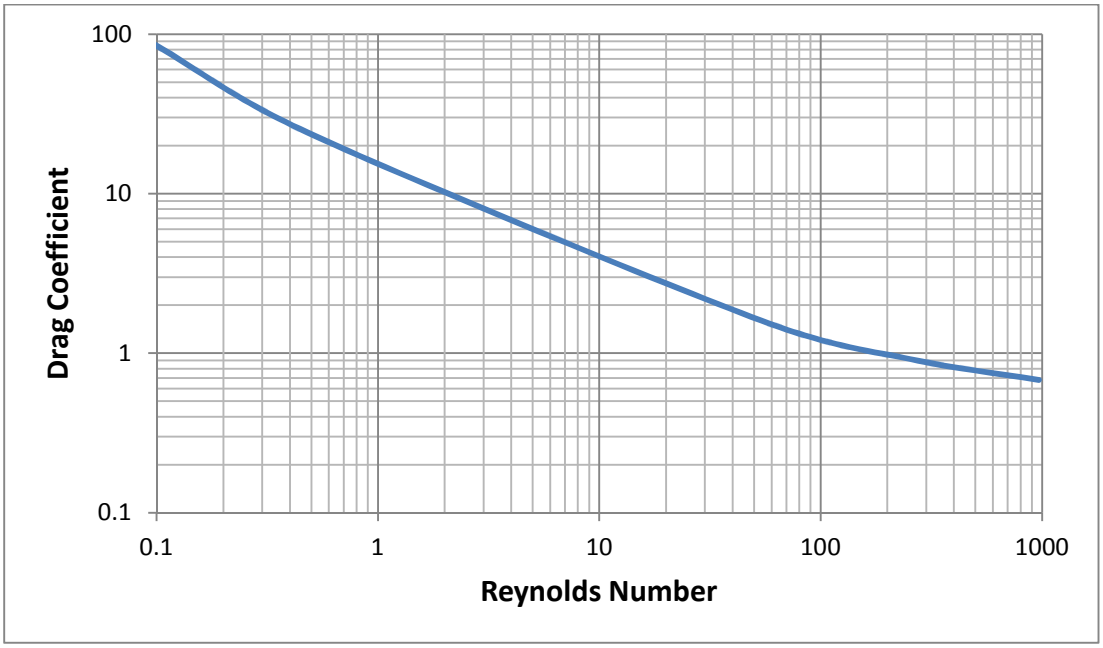

Figure 5.8: Drag Coefficient versus Particle Reynolds Number for 0.055cm particle in Non- Newtonian fluids

5.1 DISCUSSION OF RESULTS:

5.1.1 0.692 cm Particle:

From the knowledge gained in the experiment, it is observed that this particle diameter gave the highest setting velocity in both Newtonian and Non-Newtonian fluids. The reason could be the larger particles which is less affected by viscous forces and buoyancy force opposing the settling rate than the smaller particles. As such particles are much free to move faster than the smaller ones.

From the results in table 5.1 located at Appendix A and figure 5.1, it is visible that the particle Reynolds number of 0.692 cm particle diameter for the Newtonian fluids ranges from 0.82 – 1000 with a corresponding drag coefficient ranges from 33.0 – 0.408. Taking a look at the Non-Newtonian fluids, the experimental result in table 5.2 at Appendix A, and figure 5.2. Showed the particle Reynolds number in the range of 0.72 – 882 with a drag coefficient ranges from 57.19 – 0.41. In comparison between the Newtonian fluid and Non- Newtonian fluids, the drag coefficient decreases with increasing particle Reynolds number for both fluids (Zeidler, 2002). The Newtonian fluids have less drag than the Non- Newtonian fluids. The reason is that the Newtonian fluids (water) compared to the Non-Newtonian fluids, the Newtonian have a lesser viscosity (1cp) than the power law fluids (Non Newtonian) with varying viscosities which could result to increase in drag coefficient of the particle, (Dallon, 2002).

In comparison with the theoretical in the literature where experimentally, Stroke's law is found within 1% for $R_e \leq 0.1$, within 3% for $R_e \leq 0.5$ and within 9% $R_e \leq 1.0$. This is in very good agreement with the present experimental work where the Stroke drag has been determined in the range of $R_e = 0.82$ and $R_e = 0.72$ for Newtonian and Non- Newtonian fluids respectively.

The Reynolds numbers obtained fall within the limit of laminar flow region and could not produce higher Reynolds which account for the turbulent flow regime. The reason been limited experiment set up of 1m glass cylinder which could produce higher Reynolds number as one found for turbulent flow. However, the shape of the graph produce shows a resemblance with slight curve as compared to figure 2.3 and figure 2.5.

5.1.2 0.465 cm Particle:

Here the experimental results according to table 5.3 visible at Appendix A and figure 5.3 showed Reynolds number range between 0.548 – 972 and a drag coefficient of 48.07 – 0.46 for the Newtonian fluids. The Non- Newtonian Reynolds number ranges is between 0.56 – 842. The Newtonian fluids have higher Reynolds numbers with lower drag coefficient while the Non- Newtonian fluids have lower Reynolds numbers with higher drag coefficient when using the same particle. (Richard and Walker, 2001). For the Newtonian drag, inertia effect is seen to have much impact on the fluid and is responsible for the majority of force transfer to the particle.

The 0.465 cm particle settled much shower than the 0.695 cm particle. The reason could be the much effect caused by the forces opposing the settling rate of spherical particles which is resolved in figure 2.1 from the literature review.

The drag coefficient obtained from this particle particle is higher than that obtained from 0.692 cm particles in both Newtonian and non Newtonian fluids. This could be slower settling rate of particle of this type creating much drag effects in return due to the forces affecting affecting the settling rate.

In comparison with the theoretical work done in the literature, the experimental result shows good acceptability with the theoretical work of Schiller Naumaan (2001). The range of the Reynolds number obtained still falls within the laminar flow region due to the 1m cylindrical column used in performing the experiment. The shapes of figure 5.3 and figure 5.4 plotted as a result of this particle size shows a kind of resemblance with the drag figure obtained by Oseen (2000) plotted in figure 2.5.

5.1.3 0.224 cm Particle:

The small particle of this type settled much shower in comparison with 0.692cm and 0.465 cm particle. This means that lower particles have lower settling velocities than larger ones in comparison (Dallon, 2002).

Taking a look at Table 5. 4 from Appendix A and figure 5.4, it is observed that Reynolds numbers of this particle decreased more than that of 0.465 cm and 0.692 cm particles while the drag coefficient shown a higher increased than these other two particle sizes for the Newtonian fluid. But there is much drop in the particle Reynolds numbers and a tremendous rise in the drag coefficient for the Non- Newtonian fluids which is seen in table 5.5 and figures 5.5.

In the laminar slip region of these particles, the settling velocity is affected by both the rheology and the density of the fluid and settling shear rate increases.

In comparison with theoretical work, this current experimental work showed a Reynolds number of 0.068 - 876 in table 5.5 from Appendix A for the Newtonian and 0.062 – 672 for the Non- Newtonian with the resulting drag of 86.4 – 0.72 (Newtonian fluids) and 92.18- 0.83 (Non Newtonian) indicating good agreement in comparison with work done by Chabra (1990) and Oseen (2000) in correlating drag coefficient with particle Reynolds number from the literature. The shape of the figure obtained from this particle size is in slight resemblance with that obtained by Shah (1999) in figure 2.7 and figure 2.8.

5.1.4 0.055 cm Particle:

This is the smallest particle size used in this experiment. The experimental results of table 5.7, 5.8 and figure 5.7 and figure 5.8 indicated that this particle gave the highest drag coefficient for Newtonian and Non- Newtonian fluids. The observation is that the smallest particle has highest drag coefficient due to its longer time to settle (Zeidler, 2002). The settling rate of these tiny particles are longer than the previous ones due to dominant viscous buoyancy and drag forces which alters the settling rate (Richard and Walker, 2001).

The range of Reynolds numbers and drag coefficient for the Newtonian is between 0.425 – 778 and 61.5 – 0.51 respectively. While for Non- Newtonian ranges in between 0.098 – 528 and 86.09 – 0.68 respectively.

Comparing the current experimental work with the theoretical, the results obtained in table 5.7 and 5.8 showed much closeness with that obtained by (G. Mpandehis, 2001), the shape of the figures produced also showed much identical with theoretical figure of 2.4 and figure 2.3 and 2.8 respectively.

5.1.5 EFFECT OF PARTICLE SIZES

The general knowledge gained from the experiment showed that larger particles settled faster than smaller ones and larger particles have increasing settling velocity where as smaller particles yield higher drag coefficient with deceasing Reynolds numbers for both Newtonian and Non- Newtonian fluids (Maude and Whitemore, 1999).

Smaller particle sizes are much trapped by the viscous forces, buoyancy and drag forces hindering its settling rate than larger ones. The longer the particle in the fluid, the more it

become affected by these forces resisting the settling rate and the more drag coefficient it will yield (Zeidler, 2002).

5.1.6 EFFECT OF FLUID DENSITY

To inspect the effect of fluid density, medium particle size of 0.465 cm was used, maintaining the power law fluid viscosity. Particle settling velocities were high at low fluid density resulting in decreasing drag coefficient and increasing particle Reynolds numbers.

The lowest settling velocity of particles was encountered at a higher fluid density of 1.513 $glcm^3$ resulting in an increased drag coefficient and reduced particle Reynolds numbers (Zhou, 2008).

5.1.7 WALL EFFECT ON THE DRAG COEFFICIENT

Due to the presence of the wall, the confining wall exerts an extra retardation force on the particle thus the settling velocity of the particles slowed down.

Therefore, the closer the particle to the wall region, the greater will be the retardation or wall effect and consequently lower settling velocity leading to larger drag force with drag coefficient.

For all ranges of the particles small, medium or large, the drag coefficient decreases as the value of the wall factor increased (Brenner, 2001).

5.1.8 EFFECT OF VOLUMETRIC CONCENTRATION

The experimental investigation reviewed that the settling rate of particles decreased with increasing particle concentration. This phenomenon caused the drag coefficient to increase. Higher concentration of the particle tends to decrease the settling rate than the lower ones and have much influence on drag coefficient of the particles.

5.1.9 EFFECT OF TURBULENCE

According to the results obtained from the experiment which falls between the laminar flow regions. The was not much knowledge from the particle behavior from the turbulent regime, but it seems the drag coefficients will reduced for increased Reynolds number when the turbulence intensity was increased (Roberson and Rutherford, 2002). And, there will be boundary separation of fluid layers (figure 2.6)

5.2 GENERAL COMPARISON BETWEEN THE THEORETICAL, MODEL PREDICTION AND EXPERIMENTAL WORK:

After conducting the experiment, it was necessary to compare the present experimental work Theoretical work. The comparison shows some similarties with the results obtained by Schillar Naumaan (2001), Oseen (2000), Dallon (2002) and that done by Strokes.

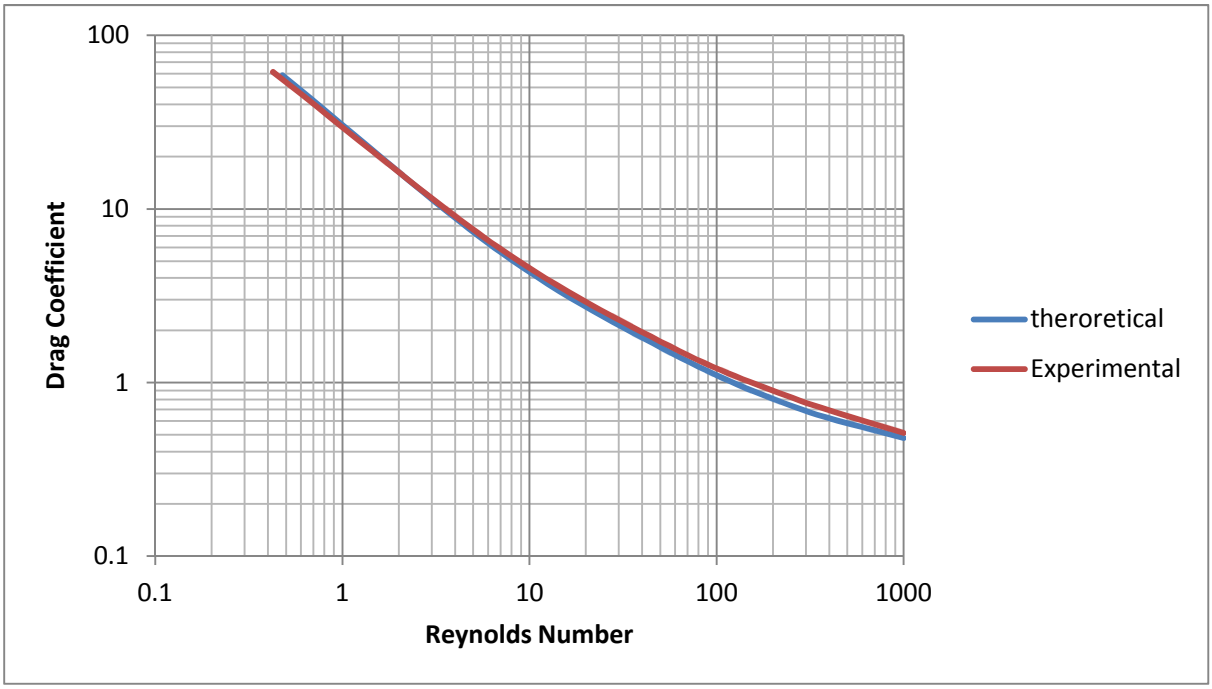

Figure 5.3.1: Comparison of Drag Coefficient versus Particle Reynolds Number between experimental and theoretical in Newtonian fluids

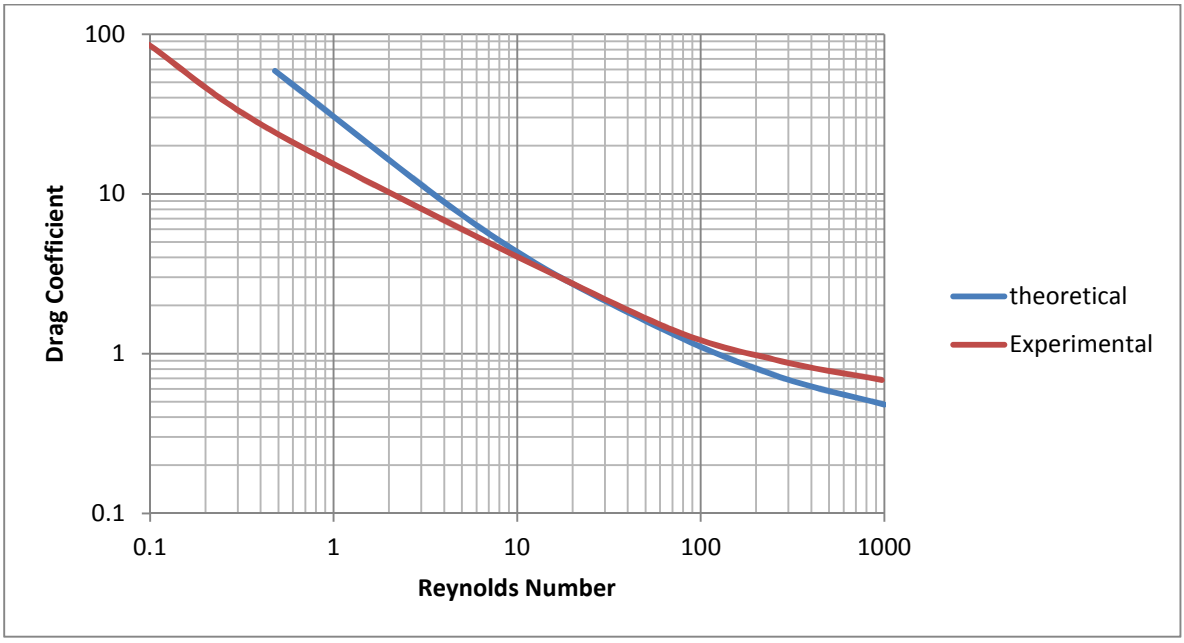

Figure 5.3.2: Comparison of Drag Coefficient versus Particle Reynolds Number between experimental and theoretical in Non - Newtonian fluids

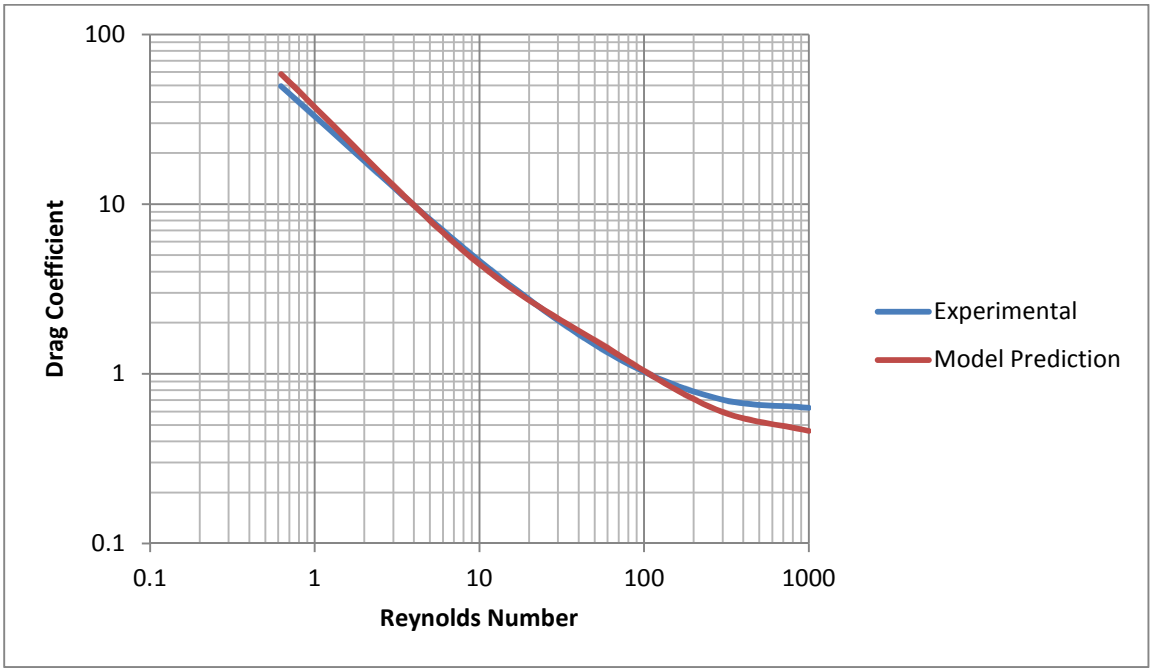

Figure 5.3.3: Model prediction compared with Experimental

The model is verified with experimental data as follows. The particle used in testing the new model correlation for drag coefficient and particle Reynolds for Newtonian fluid is 0.465 cm where the experimental result is seen in table 5.3.

Using Re = 0.548

New model correlation for drag coefficient and particle Reynolds number:

$$C_D = \frac{24}{R_{ep}} + \frac{8}{1+R_{ep}} + 0.6$$

$C_D = \frac{24}{0.548} + \frac{8}{1+0.548} + 0.6 = 49.5$

$C_D = 49.5$

Using Re = 6.82

$C_D = \frac{24}{6.82} + \frac{8}{1+6.82} + 0.6 = 5.14$

Using Re = 43.6

$C_D = \frac{24}{43.6} + \frac{8}{1+43.6} + 0.6 = 1.33$

$C_D = 1.33$

Using Re = 272.4

$C_D = \frac{24}{272.416} + \frac{8}{1+271.416} + 0.6 = 0.72$

$C_D = 0.717$

Using Re = 1000

$C_D = \frac{24}{1000} + \frac{8}{1+1000} + 0.6 = 0.63$

$C_D = 0.63$

In order to access the accuracy of the experimental work, the results obtained for Newtonian and Non- Newtonian fluids were generally compared with the theoretical values.

For the Newtonian fluids, according to the plot of 5.3.1, the plots showed that the experimental results agree with the theoretical done by Oseen (2000) .Experimental values obtained showed good similarity with that obtained from the theoretical. The shape of the figures showed some degree of likeness.

The Non- Newtonian plot is shown on figure 5.3.2. The plot also indicated satisfactory agreement between the experimental results and the theoretical results, but with only very little discrepancy in the plot. The Reynolds number ranges and the drag coefficient values also gave a very good agreement with the data for Newtonian and Non- Newtonian fluids. The plots for the Newtonian fluids showed a better similarity with the theoretical than the plot for the Non- Newtonian.

It was necessary to verify the accuracy of the new empirical correlation proposed for drag coefficient and particle Reynolds number correlation. The correlation showed similarities

with that done by Pal Skalle, Brown Lawer. The new empirical correlation also showed some kind of resemblance with that done by Clift et al.

The result from table 5.3 and figure 5.3.3 shows very satisfactory agreement with experimental data. The drag coefficient here is seen to also decrease with increasing particle Reynolds number of the same particle. The trend of their decrease also shows good agreement with the experimental data.

The shape of the graph produced from the model prediction for drag coefficient and particle Reynolds number is also in good resemblance with the one produced in the experiment data.

6.0 DISCUSSION AND EVALUATION

6.1 QUALITY OF MODEL:

The Physical model used in this work resulted in a good insight as to what really happens to cuttings particles when settling in drilling fluid during drilling operations. The existing mathematical model for estimating parameters such as settling velocity for the laminar and turbulent flow regimes were applied. New mathematical corrections for drag coefficient and particle Reynolds number were also applied for these regimes. The basic short coming of the model is that it has limited range of Reynolds Numbers captured.

6.2 QUALITY OF TEST DATA:

The test data used in this work was of considerable quality both the test conducted with water (Newtonian) and the one conducted with HEC (Non Newtonian). But the test conducted with water was of best quality due to the low viscosity easily formulated. There was a little shortcoming in the selection of the particle sizes since it was difficult to have the exact particles sizes without little mistakes. This could affect the quality of the test data. The test conducted with HEC was a bit challenging during mixing to obtain the actual HEC fluids. This could affect the quality of the test data.

Finally, the particle settling velocity was subjected to visual observations by the use of a stop watch to note the settling time, this may cause a slight error.

6.3 FUTURE IMPROVEMENT:

- This experiment and quality of the model can be improved in several ways such as:
- The experimental work was performed in the laboratory with limited number of test data, better improvement will be in the field where much test data will be involved.
- Future work is encouraged to enhance the use of the model like working with more particle settling velocity data, extending the range of the fluid behavior index, n fluid densities and particle Reynolds numbers.

- Water was used as the only fluid for the Newtonian; better improvement will involved the use of several other test fluids as the Newtonians e.g. glycerol.
- Bentonite could be a better option to produce power law fluids if there is a beam of light that can reflect the transparency of the particle when settling.
- It is hoped that, this work contributes to the Petroleum Industry for better cuttings transportation during drilling operations.

7.0 CONCLUSIONS

- Drag coefficient is influenced by surface roughness, wall effects, particle sizes, turbulence and shape, fluid properties.
- Based on the given experimental Set up, i.e. 1 m cylindrical column which could not produce larger Reynolds number for the turbulent region, the set of the Reynolds numbers produced are limited to Laminar Flow region. This affected the shape of the graph.
- The experimental work reviewed that the settling velocities of particle increased with increasing particle diameter.
- The drag coefficient of particle decreased with increasing particle Reynolds number.
- Lower particles give higher drag coefficient in result than larger ones.
- The settling velocity for a given particle decreases as the fluid becomes more viscous, therefore, the settling rate curve for the viscous fluid shifts downward as the fluid viscosity increases.
- In the laminar slip regime, settling shear rate increases with particle diameter.
- Particle settling velocities were high in higher fluids density and low at lower fluid densities.
- Wall effect has much influence on the particle settling and drag coefficient; the drag coefficient decreased as the value of the wall increases.
- Increased particle concentration and increased viscosity hinders particle settling caused the drag coefficient to increase.
- The experimental work has been compared with the theoretical and it showed good agreement.
- A new model has been developed based on the physics behind particles settling in a fluid on a force balance.
- A new empirical correlation has been developed and tested with the experimental work and it showed satisfactory agreement.

REFERENCES

Ahmed, R. 2001. Mathematical Model ling and Experimental Investigation of Solids and Cuttings Transport. PhD thesis, Norwegian University of Science and Technology, Trondheim.

Alfsen, T., Heggen, S., Blikra, H. and Tjøtta, H. 1995. Pushing the Limits for Extended Reach Drilling: New World Record from Platform Statfjord C, Well C2. SPE Dril ling & Completion, 10 (2):71–76. SPE–26350–PA.

Belavadi, M.N. and G.A. Chukwu, 1994. Experimental study of the parameters affecting cutting transportation in a vertical wellbore annulus. SPE Paper 27880. DOI: 10.2118727880-MS

Bourgoyne, A. T., Millheim, K. K., Chenevert, M. E. and Young, F. 1986. Applied Drilling Engineering, SPE Textbook Series, and Volume 2. Richardson: Society of Petroleum Engineers.

Cho, H., Shah, S.N. and Osisanya, S. O. (2002): "A three-segment hydraulic model for cuttings transport in coiled tubing horizontal and deviated drilling". J. Can. Petroleum Technol., 41: 32-39. DOI: 10.2118/02-06-03.

Clark, R. and Bickham, K. 1994. A Mechanistic Model for Cuttings Transport. Paper SPE 28306 presented at the SPE Annual Technical Conference and Exhibition, New Orleans, 25-28 September.

Darley, H. and Gray, G. 1988. Composition and Properties of Drilling and Completion Fluids, fifth edition, 5. Huston: Gulf Professional Publ.

Doan, Q., Oguztoreli, M., Masuda, Y., Yonezawa, T., Kobayashi, A., Naganawa, S. and Kamp, A. 2003. Modeling of Transient Cuttings Transport in Underbalanced Drilling (UBD). SPE Journal, 8 (2):160–170. SPE–85061–PA.

Duan, M., Miska, S., Yu, M., Takach, N., Ahmed, R. and Zettner, C. 2006. Transport of Small Cuttings in Extended-Reach Drilling. Paper SPE 104192 presented at the 2006 International Oil & Gas Conference and Exhibition, New Orleans, 5-8 October.

Fjær, E., Holt, R., Horsrud, P., Raaen, A. and Risnes, R. 2008. Petroleum Related Rock Mechanics, second edition, 2. Amsterdam: Elsevier.

Ford, J., Peden, J., Oyeneyin, M., Gao, E. and Zarrough, R. 1990. Experimental Investigation of Drilled Cuttings Transport in Inclined Boreholes. Paper SPE 20421 presented at the SPE Annual Technical Conference and Exhibition, New Orleans, 23-26 September.

Martins, A., Santana, M. and Gaspari, E. 1999. Evaluating the Transport of Solids

Generated by Shale Instabilities in ERW Drilling. SPE Dril ling & Completion, 14 (4):254–259. SPE–59729–PA.

Mims, M., Krepp, T., Williams, H. and Conwell, R. 2003. Dril ling Design and Implementation for Extended Reach and Complex Wel ls. K&M Technology Group, LLC.

Munson, B. R., Young, D. F. and Okiishi, T. H. 2002. Fundamentals of Fluid Mechanics. John Wiley & Sons, Inc.

Njaerheim, A. and Tjoetta, H. 1992. New World Record in Extended-Reach Drilling From Platform Statfjord 'C'. Paper SPE 23849 presented at the SPE/IADC Drilling Conference, New Orleans, Louisiana, 18-21 February.

Nouri, J. and Whitelaw, J. 1994. Flow of Newtonian and Non-Newtonian Fluids in an Eccentric Annulus with Rotation of the Inner Cylinder. Journal of Fluids Engineering, 116 (821):236–24

Nouri, J. and Whitelaw, J. 1997. Flow of Newtonian and Non-Newtonian Fluids in an Eccentric Annulus with Rotation of the Inner Cylinder. The International journal of heat and fluid flow, 18 (2):236–246.

Okrajni, S. and Azar, J. 1986. The Effects of Mud Rheology on Annular Hole Cleaning in Directional Wells. SPE Drilling Engineering, 1 (4):297–308. SPE–14178–PA.

Ozbayoglu, M., Saasen, A., Sorguna, M. and Svanes, K. 2007. Estimating Critical Velocity to Prevent Bed Development for Horizontal-Inclined Wellbores. Paper IADC/SPE 108005 presented at the IADC/SPE Middle East Drilling Technology Conference and Exhibition, Cairo, 22-24 October

Ozbayoglu, M.E., S.Z. Miska, T. Reed and N. Takach, 2004. Analysis of the effects of major drilling parameters on cuttings transport efficiency for high-angle wells in coiled tubing drilling operations. Proceedings of the SPE/ICoTA Coiled Tubing Conference and Exhibition, March23-24, Houston,Texas,pp:1-8.

Peysson, Y., 2004. Solid/liquid dispersions in drilling and production. Oil Gas Sci. Technol., 59: 11-21.

Peden, J., Ford, J. and Oyeneyin, M. 1990. Comprehensive Experimental Investigation of Drilled Cuttings Transport in Inclined Wells Including the Effects of Rotation and Eccentricity. Paper SPE 20925 presented at the SPE European Petroleum Conference, Hague, 22-24 October.

Saasen, A. 1998. Hole Cleaning During Deviated Drilling - The Effects of Pump Rate and Rheology. Paper SPE 50582 presented at the SPE European Petroleum Conference, Hague, 20-22 October.

Sanchez, R., Azar, J., Bassal, A. and Martins, A. 1997. The Effect of Drill pipe Rotation on Hole Cleaning during Directional Well Drilling. Paper SPE 37626 presented at the SPE/IADC Drilling Conference, Amsterdam, 4-6 March.

Sanchez, R., Azar, J., Bassal, A. and Martins, A. 1999. Effect of Drill pipe Rotation on Hole Cleaning during Directional-Well Drilling. SPE Journal, 4 (2):101–108. SPE–56406–PA
Schlumberger 2008.Oilfield Glossary. Schlumberger, www.glossary.oilfield.slb.com. Downloaded 24 March 2009.

Sifferman, T. R. and Becker, T. 1992. Hole Cleaning in Full-Scale Inclined Wellbores. Paper SPE 20422 presented at the SPE Annual Technical Conference and Exhibition, New Orleans, 23-26 September.

Simoes, S., Yu, M., Miska, S. and Takach, N. E. 2007. The Effect of Tool Joints on ECD While Drilling. Paper SPE 106647 presented at the SPE Production and Operations Symposium, Oklahoma City, 31 March-3 April.

Skalle, P. 2005. Dril ling Fluids and Borehole Hydraulics. Trondheim: Kompendiefor-Laget

Yang, W.Y., W. Cao, T. Chung and J. Morris, 2005. Applied Numerical Methods using,JohnWileyandSons,UK.,pp:179-197.

Zhou, L., 2008. Hole cleaning during underbalanced drilling in horizontal and inclined wellbore. SPE Drilling Completion, 23: 267-273.

NOMENCLATURE

A	=	Particle diameter area
A_P	=	Particle characteristic area parallel to the direction of particle motion
C_D	=	Drag coefficient
D	=	Particle diameter
F	=	Force
F_B	=	Buoyancy force
F_g	=	Gravitational force
F_D	=	Drag force
Fn	=	Resultant force
g	=	Acceleration due to gravity
k	=	Consistency index
n	=	Fluid flow behavior
R_{ep}	=	Particle Reynolds Number
V_t	=	Particle terminal velocity
$\Delta\rho$	=	Density difference
ρ_s	=	Solid density
ρ	=	liquid density
t	=	shear stress
μ	=	liquid viscosity
μ_p	=	liquid plastic viscosity

APPENDIX

APPENDIX A:

This appendix shows the result of the test carried out in the work. The results are presented in table 5.1 – 5.8: The figures shown in 5.1 – 5.8 are the plotted from these tables:

Table 5.1 : Drag coefficient and Reynolds number for 0.692 cm particles in Newtonian fluids

RE	**CD**
0.82	33.0
10.15	3.36
64.87	0.77
292.5	0.498
1000	0.408

Table 5.2 : Drag coefficient and Reynolds number for 0.692 cm particles in Non-Newtonian fluids

RE	**CD**
0.72	57.19
9.46	4.01
62.52	1.37
281.4	0.58
882	0.41

Table 5.3 : Drag coefficient and Reynolds number for 0465 cm particles Newtonian fluids

RE	CD
0.54	48.07
6.82	4.68
43.6	1.08
272.4	0.52
972	0.46

Table 5.4: Drag coefficient and Reynolds number for 0465 cm particles Non-Newtonian fluids

RE	CD
0.56	59.67
7.01	5.71
58.26	1.52
268.7	0.72
842	0.48

Table 5.5: Drag coefficient and Reynolds number 0.224 cm particles Newtonian fluids

RE	CD
0.068	86.4
0.324	23.35
51.06	1.53
240.09	0.89
786	0.72

Table 5.6 : Drag coefficient and Reynolds number for 0.224 cm particles Non-Newtonian fluids

RE	CD
0.06	92.18
0.32	26.47
48.16	1.76
19.01	0.98
672	0.83

Table 5.7 : Drag coefficient and Reynolds number for 0.055 cm particles Newtonian fluids

RE	CD
0.42	61.52
6.73	6.05
56.18	1.61
254.91	0.81
778	0.51

Table 5.8: Drag coefficient and Reynolds number for 0.055 cm particles Non- Newtonian fluids

RE	CD
0.098	86.09
0.519	23.01
54.0	1.60
252.6	0.91
528	0.68

APPENDIX B:

Table 1- 5 : Calculated results for Fluid Rheological properties

Table 1: Viscometer readings for 0.5wt% liquid HEC Polymer fluids

RPM	**SHEAR STRESS (S^{-1})**	**DIAL READING (θ)**	**SHEAR RATE (τ) Ib/100ft^2**	**SHEAR RATE(τ) Pa**
600	1022	35	37.1	17.76
300	511	26	27.56	13.20
200	341	24	25.44	12.18
100	170	15	15.9	7.61
6	10	9	9.54	4.57
3	5	7	7.42	3.55

Table 2: Viscometer readings for 1.5wt% liquid HEC Polymer fluids

RPM	**SHEAR STRESS (S^{-1})**	**DIAL READING (θ)**	**SHEAR RATE (τ) Ib/100ft^2**	**SHEAR RATE(τ) Pa**
600	1022	38	40.28	19.28
300	511	28	29.68	14.20
200	341	25	26.50	12.68
100	170	17	18.02	8.62
6	10	11	11.66	5.58
3	5	11	11.66	5.58

Table 3: Viscometer readings for 2.5wt% liquid HEC Polymer fluids

RPM	SHEAR STRESS (S^{-1})	DIAL READING (θ)	SHEAR RATE (τ) Ib/100ft^2	SHEAR RATE(τ) Pa
600	1022	44.2	46.85	22.43
300	511	30.5	32.33	15.47
200	341	26.2	27.77	13.30
100	170	18.50	19.61	9.39
6	10	12.12	12.84	6.15
3	5	11.58	12.27	5.87

Table 4: Viscometer readings for 5.0wt% liquid HEC Polymer fluids

RPM	SHEAR STRESS (S^{-1})	DIAL READING (θ)	SHEAR RATE (τ) Ib/100ft^2	SHEAR RATE(τ) Pa
600	1022	56.5	59.89	28.68
300	511	38.1	40.39	19.34
200	341	33.3	35.30	16.90
100	170	24.6	26.07	12.49
6	10	15.2	16.11	7.71
3	5	9.8	10.39	4.97

Table 5: Calculated values for rheological model for the four power law fluids

Fluid	**Rheology Model**	**Fluid Behavior Index, n**	**Consistency Index, K**
Fluid 1: HEC, 5g/liter	Power Law	0.568	0.547
Fluid 2:HEC, 2,5g/liter	Power Law	0.536	0.560
Fluid 3:HEC,1,5g/liter	Power Law	0.441	0.907
Fluid 4:HEC,0.5g/liter	Power Law	0.428	0.910

APPENDIX C:

Figures plotted from table 5.1 – 5.8

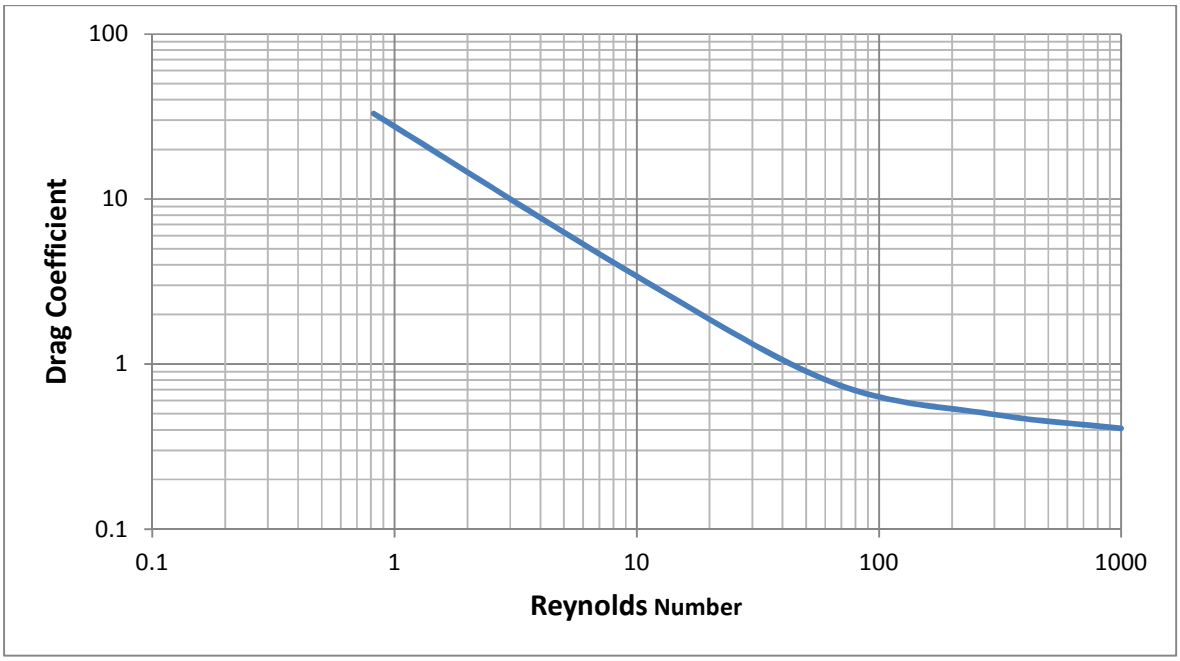

Figure 5.1: Drag Coefficient versus Particle Reynolds Number for 0.692 cm particle in Newtonian fluids

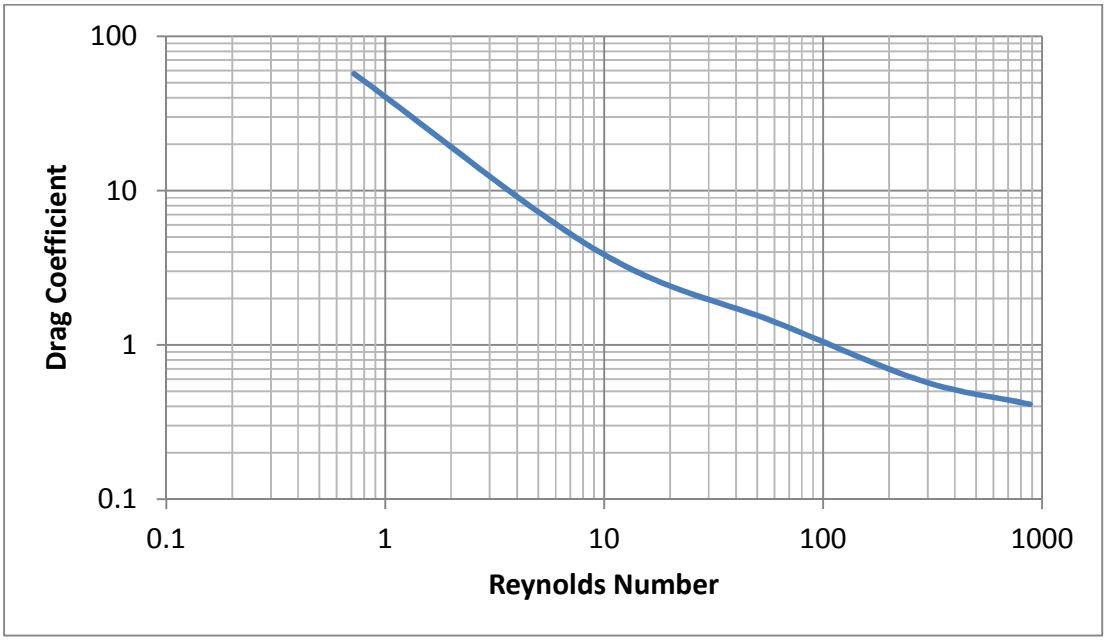

Figure 5.2: drag Coefficient versus Reynolds number for 0.692 cm in Non-Newtonian

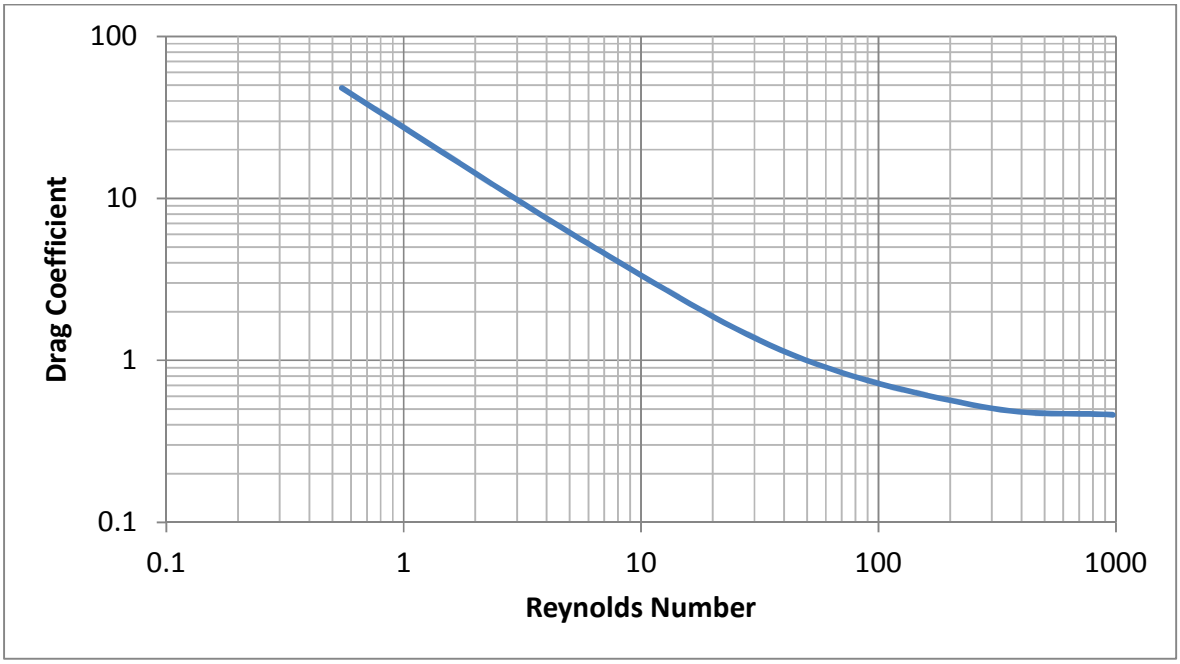

Figure 5.3: Drag coefficient versus Particle Reynolds Number for 0.465 cm particle in Newtonian

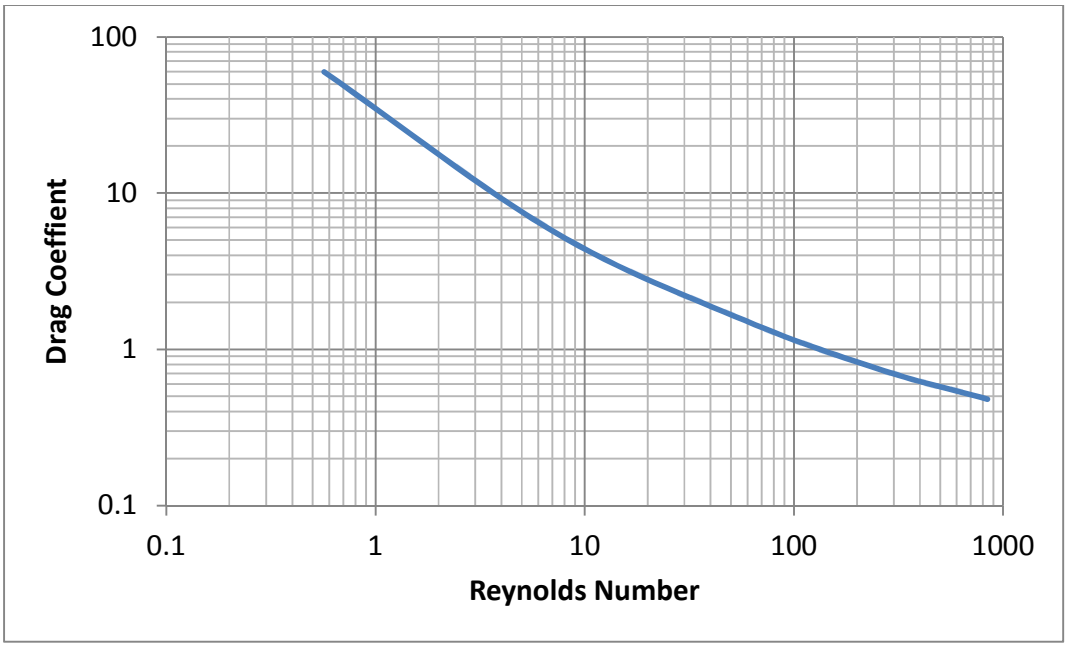

Figure 5.4: Drag Coefficient versus Particle Reynolds Number for 0.465 cm particle in Non -Newtonian fluids

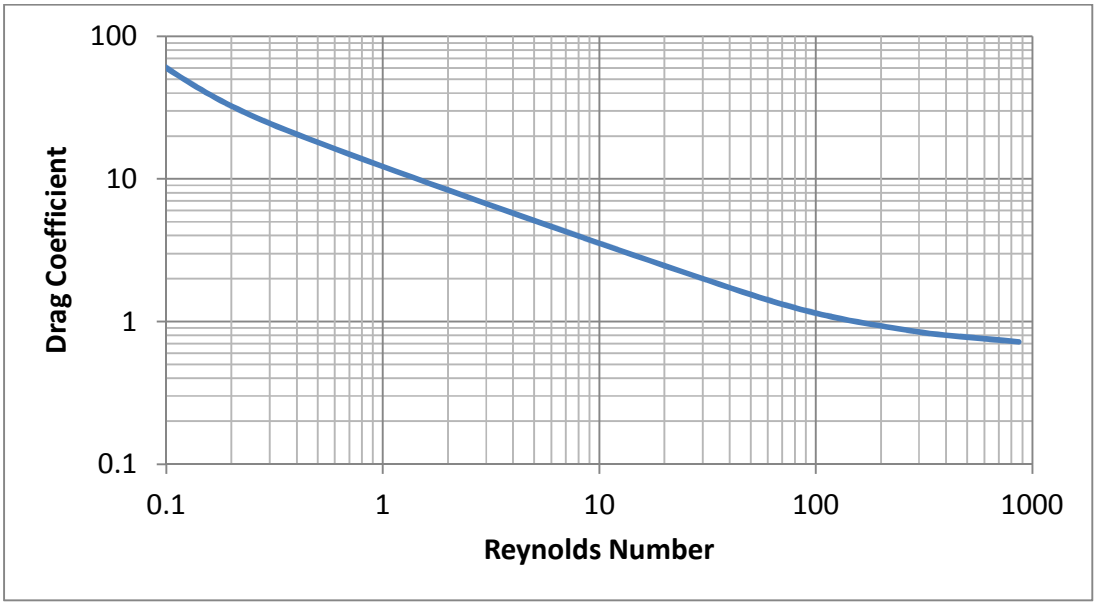

Figure 5.5: Drag Coefficient versus Reynolds number for o.224 cm particle in Newtonian

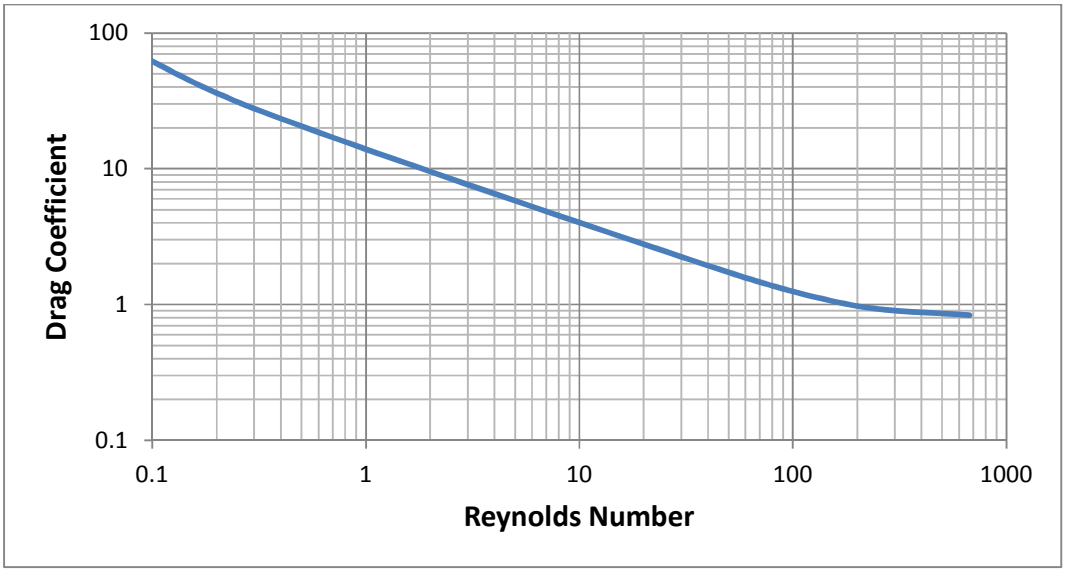

Figure 5.6: Drag Coefficient versus Particle Reynolds Number for 0.224 cm particle in Non-Newtonian fluids

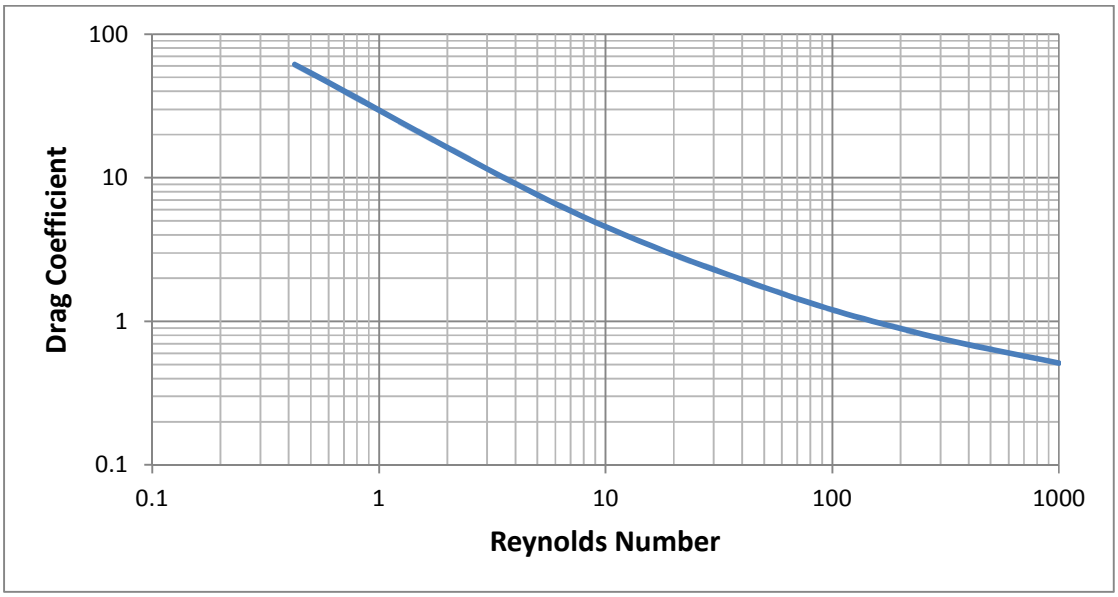

Figure 5.7: Drag Coefficient versus Particle Reynolds Number for 0.055 cm particle in Newtonian fluids

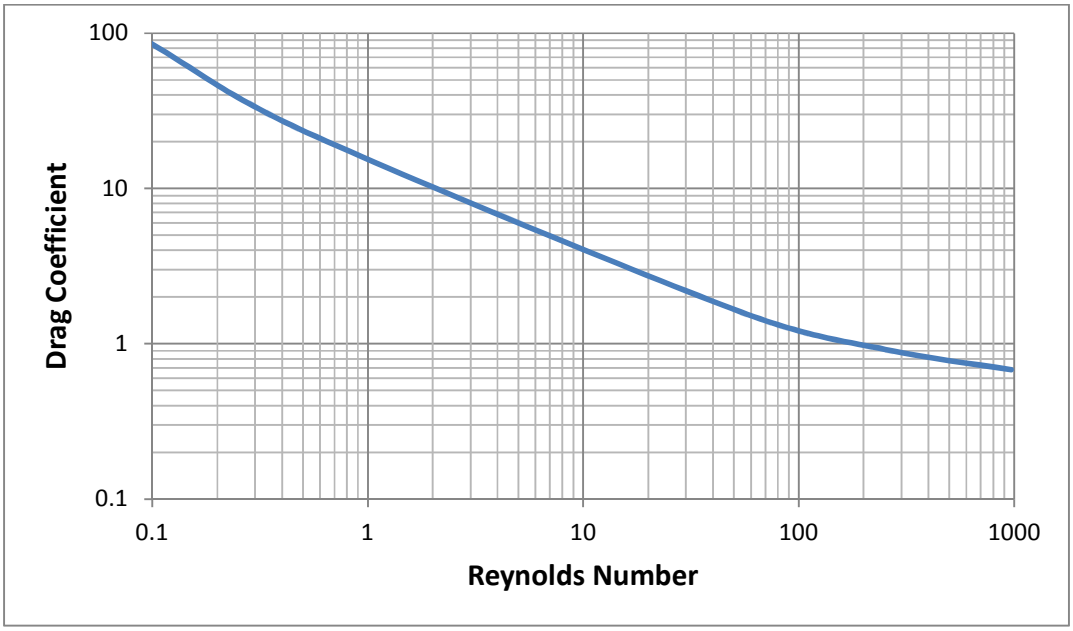

Figure 5.8: Drag Coefficient versus Particle Reynolds Number for 0.055 cm particle in Non- Newtonian fluids

APPENDIX D:

Sample of Experimental set up

APPENDIX E

DRAG COEFFICIENT VERSUS REYNOLDS NUMBER COMPARISON:

YEAR	INVESTIGATOR	$C_D - R_e$ relationship
1997	Brown and Lawer	$C_D = \frac{24}{R_e}(1 + 0.15\,R_e^{0.681}) + \frac{0.407}{1+8710\,R_e^{-1}}$ for $R_{e<2\,x\,10^5}$
2001	Clift *et al.*	$C_D = 24/R_e$ 3/16 for $R_e < 0.01$
2003	Clift and Gauvin	$C_d\ \frac{24}{R_e}(1 + 0.15R_e^{0.687}) + \frac{0.42}{1 + 22500\,R_e^{-1.16}}$
2004	Flemmer and Banks	$C_d = \frac{24}{R_e}\,10^{\propto}\ for\ R_e < 3\ x\ 10^5, where\ \propto = 0.261R_e^{0.369} - 0.105R_e^{0.431} - \frac{0.124}{1+log^2\,R_e}$
2006	Turton and Levenspiel	$C_d = \frac{24}{R_e}(1 + 0.173R_e^{0.657}) + \frac{0.413}{1+16300\,R_e^{-1.09}}$ for $R_e < 2$ x 10^5